104
27

PARAMETER IDENTIFICATION IN DISTRIBUTED STRUCTURES

by

Mark A. Norris

Dissertation submitted to the faculty of the

Virginia Polytechnic Institute and State University

in partial fulfillment of the requirements for the degree of

DOCTOR OF PHILOSOPHY

in

Engineering Mechanics

APPROVED:

Dr. L. Meirovitch, (Chairman)

Dr. S. L. Hendricks

Dr. D. Frederick

Dr. D. T. Mook

Dr. H. F. VanLandingham

September, 1986

Blacksburg, VA

PARAMETER IDENTIFICATION IN DISTRIBUTED STRUCTURES

by

Mark A. Norris

Committee Chairman: Leonard Meirovitch
Engineering Science and Mechanics

(ABSTRACT)

This dissertation develops two new techniques for the identification of parameters in distributed-parameter systems. The first technique identifies the physical parameter distributions such as mass, damping and stiffness. The second technique identifies the modal quantities of self-adjoint distributed-parameter systems.

Distributed structures are distributed-parameter systems characterized by mass, damping and stiffness distributions. To identify the distributions, a new identification technique is introduced based on the finite element method. With this approach, the object is to identify "average" values of mass, damping and stiffness distributions over each finite element. This implies that the distributed parameters are identified only approximately, in the same way in which the finite element method approximates the behavior of a structure.

It is common practice to represent the motion of a distributed-parameter system by a linear combination of the associated modes of vibration. In theory, we have an infinite set of modes although, in practice we are concerned with only a finite linear combination of the modes. The modes of vibration possess certain properties which distinguish them from one another. Indeed, the modes of vibration are

uncorrelated in time and orthogonal in space. The modal identification technique introduced in this dissertation uses both these spatial properties. Because both the temporal and spatial properties are used, the method does not encounter problems when the natural frequencies are closely-spaced or repeated.

ACKNOWLEDGEMENTS

I am highly indebted to my major advisor, Professor Leonard Meirovitch, for his guidance and support throughout my undergraduate and graduate studies. Indeed, I was very honored to have been able to work under his guidance. Furthermore, his task of identification of my career interests and implementing the control of the fruitful research activities is greatly appreciated.

I would also like to thank my graduate committee members, Professor D. Frederick, S. L. Hendricks, D. T. Mook and H. F. VanLandingham, as well as former members, Professors J. L. Junkins and R. H. Plaut for their guidance.

I would like to attempt to thank my parents, and Norris, with whose guidance, support and love have made this possible.

Last but not least, I would like to thank and for their patience and politeness in the expert typing of this dissertation.

TABLE OF CONTENTS

LIST OF FIGURES

LIST OF TABLES

Chapter 1

INTRODUCTION

The motion of a distributed structure is governed by partial differential equations (PDEs) where the parameters, namely the mass, damping and stiffness distributions, are continuous functions of the spatial variables. In practice, it is often necessary to eliminate the spatial dependence through discretization, where the infinite number of degrees of freedom system is approximated by a finite one. A common tool for discretization of distributed structures is the finite element method, which can be regarded as a variant of the Rayleigh-Ritz method. The method is based on a variational principle, and under certain conditions the approximate solution converges to the actual solution.

Of particular interest are large space structures (LSS) whose proposed missions require active control for maneuvering and vibration suppression. Before satisfactory controls can be designed, it is necessary to know certain parameters quite accurately. These parameters are the mass, damping and stiffness distributions and the modal quantities. To determine these parameters, one must elicit the system response and use this information to deduce the system parameters. This is the problem of parameter identification.

The problem of identifying parameters of distributed structures has received considerable attention in recent years [1-42]. Surveys relevant to the identification of parameters in distributed structures can be found in Refs. 1-4. As discussed in Ref. 4, the structural identification techniques can be broadly classified into direct and indirect methods. However, to stress the importance of identifying distributed

parameters, we include a third category, namely, identification of parameters in distributed systems.

The first approach is the indirect approach, whereby the modal quantities associated with the actual distributed system are identified first and then use is made of this modal information to identify the system parameters [5-14]. However, modal data cannot uniquely determine the lumped-parameter model unless some a priori information is known about the mass and stiffness matrices [5,6]. Indeed, in order to compute the response of the system, it is necessary to know the mass distribution, in addition to the modal data. Early approaches for identifying eigenvalues and eigenvectors used near-resonance testing [7]. Difficulties arise for this type of approach when the natural frequencies are repeated or closely-spaced [5,8].

Reference 9 uses a Jacobian or sensitivity matrix to recursively update the system parameters based on modal test results. It describes a matrix perturbation method to compute the Jacobian matrix and presents a numerical example having 84 degrees of freedom. The method requires that the number of estimated parameters must be equal to (or less than) the number of modal parameters. This work has been advanced in Ref. 10, where the Gaussian least-squares differential correction algorithm [43] is used to obtain a best estimate of the structural parameters. The authors stress the importance of identifying physical parameters such as moduli of elasticity, mass densities, spacecraft dimensions, etc., rather than entries in mass and stiffness matrices.

As another example of the indirect method, Ref. 11 identifies mass and stiffness distributions of distributed structures using an indirect

approach. Indeed, the mass and stiffness distributions are expressed in the form of series of known functions multiplied by unknown coefficients. The unknown coefficients are determined by making use of the identified modal quantities. References 12-14 use the identified modal quantities to improve a priori mass, damping and stiffness matrices.

The second approach identifies the distributed model by identifying the spatial functions in the partial differential equations of motion [15-18]. Reference 15 expresses the system operator in terms of known operators with unknown coefficients. The unknown coefficients are determined recursively by a perturbation method. Reference 16 uses a Green's function approach to obtain integral equations that can be solved for unknown spatial operators or coefficients. Reference 17 uses the same approach combined with an optimality criterion for control and estimation of static models. The identification schemes [15-17] are described for distributed systems where the system parameters are not complicated functions of the spatial variable. However, in general the system parameters tend to be complicated functions of the spatial variable. Hence, we must resort to spatial discretization methods, such as the finite element method.

Identification using continuum models is a subject of current interest [18]. Several methods have been proposed to construct continuum models to represent discrete structures such as trusses [44-47]. Many large truss structures function as beams or plates. Hence, in certain cases modeling discrete structures as continua has practical applications. Reference 18 identifies parameters of discrete structures

by using simple continuum models; i.e., uniform beams and plates. The identified parameters are uniform mass and stiffness distributions.

The third approach identifies directly modal quantities or mass, damping and stiffness matrices associated with ordinary differential equations of motion describing lumped systems [19-42]. The approach uses time and frequency domain techniques to identify the parameters. References 19-37 identify modal quantities of structures, whereas Refs. 38-42 identify coefficient matrices.

A time-domain identification scheme was developed in Refs. 19-21 where the modal parameters of lumped models are identified. The method requires sensor measurements at each degree of freedom and has been shown to successfully identify modal parameters of complex structures [22,23]. Reference 24 identifies the modal parameters for distributed structures using a modified version of the Ibrahim time-domain method.

Reference 25 identifies the order of the system as well as the eigendata using lattice filters. The lattice filters determine the order of the system and form an orthonormal basis spanning the motion of the system using a Gram-Schmidt procedure. Then, the basis vectors are decoupled by a fast Fourier transform to produce the eigenvectors of the system. An example using the flexible beam at NASA Langley illustrates the procedure.

References 26 and 27 use the Ho-Kalman algorithm in conjunction with a singular value decomposition technique to identify a linear state-space model of minimum order. The identified state-space model is then transformed into the modal-space for modal parameter identification. The algorithm has been shown to work well [27], but the

algorithm's efficiency is questionable. Nearly 10 minutes of CPU time were required on a CDC mainframe to compute 20 modes of a 162 order model.

References 28 and 29 use frequency-domain data to identify modal parameters of structures. For lightly damped structures, Ref. 28 discusses a technique to identify the normal modes. For more heavily damped structures, Ref. 29 introduces methods to identify complex modes.

The majority of the direct time-domain methods for system parameter identification consider the system input and output to be stochastic and use auto regressive (AR) models, autoregressive moving average (ARMA) models, maximum likelihood estimation, generalized least-squares, Bayesian estimation (for stochastic systems) and optimality criterion [30-37]. As an example, Ref. 30 uses AR and ARMA models to predict the frequencies and damping ratios for a given transfer function. The order of the AR and ARMA models are at least 3 times the order of the identified transfer function for permissible results. In general, these techniques are implemented only for low-order discrete systems. However, the order and number of identified transfer functions for distributed structures can be very large. Indeed, distributed structures possess an infinity of transfer functions. The approach of this dissertation is to solve the simpler deterministic problem first and then to include stochastic effects caused by actuator and sensor noise.

Reference 38 uses a frequency-domain method to identify directly the mass, damping and stiffness matrices from measured system responses and system inputs. The differential equation of motion is formulated in the frequency domain such that the parameters are the unknowns. In

general, the number of equations exceeds the number of unknowns and the coefficient matrix is ill-conditioned by the fact that it contains response data corresponding to high frequencies. The authors stress that a least-squares technique is ineffective in this case. However, a method using Householder's transformation does not give rise to numerical difficulties. The results in this dissertation did not require Householder's method. Reference 38 identifies entries in mass, damping and stiffness matrices, whereas this dissertation identifies approximate values of mass, damping and stiffness distributions, which implies a smaller number of parameters to be identified.

Reference 39 identifies the physical parameters entering into tridiagonal damping and stiffness matrices of a lumped-parameter model. Reference 38 estimates mass, damping and stiffness matrices of lumped models using the frequency response, whereas Refs. 40-42 identify mass, damping and stiffness matrices in the time domain. The approaches in Refs. 38-42 require measurements at each degree of freedom entering into the equations of motion. The procedures are more suitable for lumped-parameter systems than for distributed systems, as mass, damping, and stiffness matrices are not unique for a distributed structure. Even for lumped systems, it is likely to be more efficient to identify the physical parameters of the structure directly, as entries in the mass, damping and stiffness matrices are functions of these parameters and there are fewer parameters than entries in the matrices, which implies that these entries are not independent but constrained. Indeed, Ref. 39 identifies N damping and N stiffness parameters, while the symmetric damping and stiffness matrices contain $(N+1)\times N/2$ entries each. Hence,

for this lumped system, it is more efficient to identify the physical parameters of the structure directly.

This dissertation develops a new technique for the approximate identification of mass, damping and stiffness distributions in distributed structures. The technique is based on the finite element method and the object is to identify "average" values of mass, damping and stiffness distributions over each finite element. Hence, the scheme represents physical parameter identification in a finite element sense. This implies that the distributed parameters are identified only approximately, in the same way in which the finite element method approximates the behavior of a distributed structure. References 10 and 39 also seek to identify physical parameters, but the parameters are lumped in nature, whereas for distributed structures they are distributed. This dissertation also shows that the algorithm may work with an incomplete set of measurements. Whereas Refs. 41 and 42 consider an incomplete set of measurements, they require at least one measurement at each degree of freedom in the lumped model.

Chapter 2 of the dissertation presents the equations of motion for a distributed structure and the finite element equations of motion. Parameter identification of distributed spacecraft structures is the topic of Chapter 3. Chapter 4 presents the algorithm in recursive form using the frequency domain. In this approach, a reduced number of sensor measurements is used to identify the parameters. Chapter 5 introduces a modal identification technique. Numerical examples are presented at the ends of Chapters 3, 4 and 5.

Chapter 2

EQUATIONS OF MOTION FOR DISTRIBUTED STRUCTURES

Distributed structures represent distributed-parameter systems (DPS), which implies that the mass and stiffness properties depend on the spatial variables. The motion of a damped DPS can be written in the form of the partial differential equation [49, Ch. 9, Sec. 12]

$$m(P)\partial^2 u(P,t)/\partial t^2 + \partial[Cu(P,t)]/\partial t + Lu(P,t) = f(P,t) \qquad (2.1)$$

which much be satisfied at every point P in the domain D of the system, where

$u(P,t)$ = displacement at point P and time t

$m(P)$ = distributed mass

C = linear time-invariant differential operator of order 2p, expressing the system damping

L = linear positive semidefinite self-adjoint differential operator of order 2p, expressing the system stiffness

$f(P,t)$ = distributed force

The displacement $u(P,t)$ is subject to the boundary conditions

$$B_i u(P,t) = 0, \quad i = 1,2,\ldots,p \qquad (2.2)$$

to be satisfied at every point on the boundary S of the domain D, where $B_i (i = 1,2,\ldots,p)$ are linear differential operators of order ranging from zero to 2p-1. The boundary conditions are either geometric, in which case the order of B_i is no greater than p, or natural, in which case the order of B_i is greater than p. Functions satisfying the geometric boundary conditions are called admissible functions [49].

Associated with Eq. (2.1), we have the eigenvalue problem

$$L\phi_r(P) = \lambda_r m(P)\phi_r(P), \quad r = 1,2,\ldots \qquad (2.3)$$

where the functions $\phi_r(P)$ $(r = 1,2,...)$ satisfy the boundary conditions given in Eq. (2.2). The solution to Eq. (2.3) consists of a denumerably infinite set of real eigenfunctions $\phi_r(P)$ and associated real non-negative eigenvalues λ_r $(r = 1,2,...)$. For convenience, we order the eigenvalues so that $\lambda_1 \leq \lambda_2 \leq \lambda_3 \ldots$. The infinite set of eigenfunctions is orthogonal and can be normalized so as to satisfy the orthonormality conditions

$$\int_D m(P)\phi_r(P)\phi_s(P)dD = \delta_{rs}, \quad \int_D \phi_r(P)L\phi_s(P)dD = \lambda_r\delta_{rs} \tag{2.4}$$

where δ_{rs} is Kronecker delta.

The eigenfunctions ϕ_r form a complete set. Hence, any function in the Sobolev space K_B^{2p} satisfying all the boundary conditions and possessing 2p derivatives can be expressed as [50]

$$u(P,t) = \sum_{r=1}^{\infty} \phi_r(P)u_r(t) \tag{2.5}$$

where the $u_r(t)$ are generalized coordinates.

Equation (2.5) represents the expansion theorem for continuous systems. Introducing Eq. (2.5) into (2.1), multiplying by ϕ_s and taking into account Eqs. (2.4), we obtain

$$\ddot{u}_r(t) + \sum_{s=1}^{\infty} c_{rs}\dot{u}_s(t) + \omega_r^2 u_r(t) = f_r(t), \quad r = 1,2,... \tag{2.6}$$

where

$$c_{rs} = \int_D \phi_r C\phi_s dD, \quad r,s = 1,2,... \tag{2.7}$$

are damping coefficients and

$$f_r(t) = \int_D \phi_r(P)f(P,t)dD \tag{2.8}$$

are modal forces.

Equations (2.6) represent an infinite set of ordinary differential equations. Note that in general damping recouples these equations. Various mechanisms for damping exist, but ordinarily high-strength structural materials have relatively small internal friction [51]. This implies that LSS will have relatively small damping. Hence, we assume that the damping is light and an approximate solution is obtained by considering the coupling due to damping as a secondary effect [49]. Ignoring coupling due to damping, we can write Eq. (2.7) as

$$c_{rs} = \int_D \phi_r C \phi_s dD = 2\zeta_r \omega_r \delta_{rs} \tag{2.9}$$

Substituting Eq. (2.9) into (2.6), we obtain

$$\ddot{u}_r(t) + 2\zeta_r \omega_r \dot{u}_r(t) + \omega_r^2 u_r(t) = f_r(t), \quad r = 1,2,... \tag{2.10}$$

Finite Element Equations of Motion

The finite element method is a discretization (-in-space) procedure capable of approximating the partial differential equation, Eq. (2.1), by a set of simultaneous ordinary differential equations. Because this set has finite dimension, the finite element method is a truncation procedure at the same time. For simplicity, we consider a one-dimensional structure, so that P = x in equation (2.1). Moreover, the domain D of the structure is $0 < x < L$, where L is the length. Then, we divide the structure into N subdomains of width $h = L/N$ (Fig. 1), where the subdomains are the finite elements, and denote by m_j, c_j and k_j the "average" values of the mass, damping and stiffness distributions over a typical element j. The displacement $w(x,t)$ inside the finite element can be expressed in terms of displacements at the boundaries of the element as follows [50]:

$$w(x,t) = \underset{\sim}{\phi}^T(x)\underset{\sim}{w}_j(t) \quad , \quad (j-1)h \le x \le jh \quad , \quad j = 1,2,\ldots,N \tag{2.11}$$

where $\underset{\sim}{\phi}(x)$ is a vector of interpolation functions and $\underset{\sim}{w}_j(t)$ is a vector of "nodal" displacements (Fig. 2). The term nodal derives from the fact that in finite element terminology the boundary points are called nodes. By letting the magnitude of the interpolation functions and their first derivatives be equal to either zero or one at the nodes, one makes the nodal coordinates represent the actual coordinates of the structure at the nodal points.

Following the usual steps [50], we obtain the element mass, damping and stiffness matrices

$$M_j = \int_{(j-1)h}^{jh} m\underset{\sim}{\phi}\underset{\sim}{\phi}^T \, dx \cong m_j \int_{(j-1)h}^{jh} \underset{\sim}{\phi}\underset{\sim}{\phi}^T \, dx = m_j \Phi_M, \quad j = 1,2,\ldots,N \tag{2.12a}$$

$$C_j = \int_{(j-1)h}^{jh} (C\underset{\sim}{\phi})\underset{\sim}{\phi}^T \, dx \cong c_j \Phi_C, \quad j = 1,2,\ldots, N \tag{2.12b}$$

$$K_j = \int_{(j-1)h}^{jh} (L\underset{\sim}{\phi})\underset{\sim}{\phi}^T dx = [\underset{\sim}{\phi},\underset{\sim}{\phi}]_j \cong k_j \Phi_K, \quad j = 1,2,\ldots,N \tag{2.12c}$$

where m_j, c_j and k_j ($j = 1,2,\ldots,N$) are average values of the mass, damping and stiffness distributions for element j, respectively, and $[\ ,\ ]_j$ represents the energy inner product defined over element j. (For details on the use of the interpolation functions entering into the energy inner product, see [50].) Note that Φ_M, Φ_C and Φ_K are element matrices computed by substituting the given interpolation functions into Eqs. (2.12) and they are the same for every element [50].

The global mass, damping and stiffness matrices, M, C and K respectively, are obtained by carrying out the so-called assembling process [50], which represents the transition from the individual finite elements to the whole structure. As shown in [50], the equations of motion have the form

$$\underset{\sim}{M}\ddot{\underset{\sim}{w}} + \underset{\sim}{C}\dot{\underset{\sim}{w}} + \underset{\sim}{K}\underset{\sim}{w} = \underset{\sim}{F} \tag{2.13}$$

The global mass matrix M is obtained through a superposition of element matrices M_j. The superposition is such that the entries in two adjacent matrices corresponding to the shared nodal displacements overlap. The global mass matrix has the form

$$M = \begin{bmatrix} M_1 & & & & \\ & M_2 & & & \\ & & M_3 & & \\ & & & \ddots & \\ & & & & M_{N-1} \\ & & & & & M_N \end{bmatrix} \tag{2.14}$$

and it represents the n×n mass matrix for the whole structure. The overlapping entries, marked by shading in equation (2.14), are obtained by the addition of the corresponding entries in two adjacent element mass matrices. The n×n damping matrix C and stiffness matrix K have block-diagonal forms similar to that of M.

Chapter 3

PARAMETER IDENTIFICATION IN DISTRIBUTED SPACECRAFT STRUCTURES

The chapter first presents the parameter identification method referring to the equations of motion derived in Chapter 2. Then, some concepts relevant to the identification of space structures are introduced. To illustrate the technique, a numerical example is presented in which the mass and stiffness distributions of a space structure, simulated by a nonuniform free-free beam, are identified.

The Parameter Identification Process

The parameter identification process consists of exciting the structure by means of known nodal forces and measuring the response. Because the excitation and response are known, Eq. (2.13) can be regarded as a set of simultaneous algebraic equations in the system parameters, and can be solved by a least-squares technique. To this end, we introduce the $n \times 3n$ matrix

$$L = [M \quad C \quad K] \tag{3.1}$$

and the 3n-dimensional vector

$$\underset{\sim}{x}(t) = [\ddot{\underset{\sim}{w}}^T(t) \quad \dot{\underset{\sim}{w}}^T(t) \quad \underset{\sim}{w}^T(t)]^T \tag{3.2}$$

In terms of this notation, Eq. (2.13) can be rewritten in the form

$$L\underset{\sim}{x}(t) = \underset{\sim}{F}(t) \tag{3.3}$$

Next, we denote the system parameters

$$p_r = \begin{cases} m_r, & 1 \le r \le N \\ c_{r-N}, & N+1 \le r \le 2N \\ k_{r-2N}, & 2N+1 \le r \le 3N \end{cases} \tag{3.4}$$

and observe that the matrix L can be rewritten as

$$L = \sum_{r=1}^{3N} \frac{\partial L}{\partial p_r} p_r \tag{3.5}$$

where

$$\frac{\partial L}{\partial p_r} = \begin{cases} \left[\frac{\partial M}{\partial m_r} \quad 0 \quad 0\right] = \left[\Phi_M' \quad 0 \quad 0\right], & 1 \le r \le N \\ \left[0 \quad \frac{\partial C}{\partial c_{r-N}} \quad 0\right] = \left[0 \quad \Phi_C' \quad 0\right], & N+1 \le r \le 2N \\ \left[0 \quad 0 \quad \frac{\partial K}{\partial k_{r-2N}}\right] = \left[0 \quad 0 \quad \Phi_K'\right], & 2N+1 \le r \le 3N \end{cases} \tag{3.6}$$

where it follows from Eqs. (2.12a) and (2.14) that Φ_M' is an $n \times n$ matrix with Φ_M occupying the block corresponding to M_r and with zero entries everywhere else. The matrices Φ_C' and Φ_K' are defined similarly. Hence, Eq. (3.3) can be expressed explicitly in terms of the system parameters as follows:

$$\sum_{r=1}^{3N} \left[\frac{\partial L}{\partial p_r} \underset{\sim}{x}(t)\right] p_r = \underset{\sim}{F}(t) \tag{3.7}$$

But, $(\partial L/\partial p_r)\underset{\sim}{x}(t)$ is an n-dimensional vector of the form

$$\frac{\partial L}{\partial p_r} \underset{\sim}{x}(t) = \underset{\sim}{a}_r(t) \tag{3.8}$$

where

$$\underset{\sim}{a}_r(t) = \Phi_M' \ddot{\underset{\sim}{w}}(t) = \begin{bmatrix} 0 \\ 0 \\ \Phi_M \ddot{w}_r(t) \\ 0 \\ 0 \end{bmatrix}, \quad 1 \le r \le N \tag{3.9a}$$

$$\underset{\sim}{a}_r(t) = \Phi_C' \dot{\underset{\sim}{w}}(t) = \begin{bmatrix} 0 \\ 0 \\ \Phi_C \dot{w}_{r-N}(t) \\ 0 \\ 0 \end{bmatrix}, \quad N+1 \le r \le 2N \tag{3.9b}$$

$$\underset{\sim}{a}_r(t) = \Phi_K' \underset{\sim}{w}(t) = \begin{bmatrix} 0 \\ 0 \\ \Phi_K w_{r-2N}(t) \\ 0 \\ 0 \end{bmatrix}, \quad 2N+1 \le r \le 3N \tag{3.9c}$$

Then, introducing the notation

$$A(t) = [\underset{\sim}{a}_1(t)\ \underset{\sim}{a}_2(t)\cdots\underset{\sim}{a}_{3N}(t)] \tag{3.10a}$$

$$\underset{\sim}{p} = [p_1\ p_2\cdots p_{3N}]^T \tag{3.10b}$$

where $A(t)$ is an $n \times 3N$ matrix of coefficients and $\underset{\sim}{p}$ is a 3N-dimensional vector of parameters, inserting Eq. (3.8) into Eq. (3.7) and considering Eqs. (3.10), we obtain

$$A(t)\underset{\sim}{p} = \underset{\sim}{F}(t) \tag{3.11}$$

which represents the desired equations with the system parameters as unknowns. To extract the system parameters from Eq. (3.11), we consider the sampling times $t = t_k$ $(k = 1,2,\ldots, m)$ and write

$$A(t_k)\underset{\sim}{p} = \underset{\sim}{F}(t_k),\ k = 1, 2,\ldots, m \tag{3.12}$$

Equations (3.12) represent a set of $n \cdot m$ algebraic equations and 3N unknowns. To solve the equations it is convenient to introduce the notation

$$B = \begin{bmatrix} A(t_1) \\ A(t_2) \\ \vdots \\ A(t_m) \end{bmatrix}, \quad \underset{\sim}{c} = \begin{bmatrix} \underset{\sim}{F}(t_1) \\ \underset{\sim}{F}(t_2) \\ \vdots \\ \underset{\sim}{F}(t_m) \end{bmatrix} \tag{3.13a,b}$$

where B is an $n \cdot m \times 3N$ matrix and $\underset{\sim}{c}$ is an $n \cdot m$-dimensional vector, so that Eqs. (3.12) can be combined into

$$B\underset{\sim}{p} = \underset{\sim}{c} \tag{3.14}$$

In general, $n \cdot m > 3N$ so that the solution of Eq. (3.14) can be obtained by a least-squares algorithm [43]. The result is

$$\underset{\sim}{p} = (B^TB)^{-1}B^T\underset{\sim}{c} \tag{3.15}$$

where B^TB is guaranteed to be nonsingular if B has maximum rank, namely, 3N.

Parameter Identification in Spacecraft Structures

The equations of motion of a spacecraft free to move in space are linear provided the rigid-body rotational motion is small. Hence, in the identification process the excitation forces must be such that the rotational motion is not significantly excited.

The parameter identification process works provided the response does not consist of rigid-body motion alone. Indeed, the matrix B(t) in Eq. (3.13a) does not have maximum rank when only rigid-body motion is excited. The stiffness matrix in the case of a spacecraft capable of undergoing rigid-body motions is positive semidefinite. The vector $\underset{\sim}{a}_r(t)$ $(2N + 1 < r < 3N)$ in Eq. (3.9c) is orthogonal to the nodal displacement vector $\underset{\sim}{w}(t)$ when the motion is due entirely to rigid-body displacements. Hence, a necessary condition for the matrix B(t) to have maximum rank is that the elastic motion participate in the response.

The method is stable in the presence of measurement noise. To determine the effect of noise, the numerical example includes random noise in the nodal forces and in the measurements of the nodal accelerations; the nodal velocities and displacements are obtained by integrating the nodal accelerations. The effect of the noise can be reduced by increasing the number of sampling instances m in Eqs. (3.13).

Numerical Example

We consider a free-free nonuniform beam (Fig. 3.1) undergoing translational and rotational rigid-body motions in addition to bending vibration. The energy inner product in Eq. (2.12c) has the form [50]

$$[w, w]_j = \int_{(j-1)h}^{jh} EI(x) \left[\frac{\partial^2 w(x,t)}{\partial x^2} \right]^2 dx \tag{3.16}$$

where EI is the flexural rigidity. In the finite element model for a beam in bending, the nodal displacements are the transverse displacement and rotation at each node. From Eq. (3.16), we conclude that both the displacement and its first derivative must be continuous over the spatial domain. The indicated interpolation functions used in Eq. (2.11) are Hermite cubics. In terms of local coordinates, the interpolation functions are [50]

$$\phi_1 = 3\xi^2 - 2\xi^3 \quad , \quad \phi_2 = \xi^2 - \xi^3$$
$$\phi_3 = 1 - 3\xi^2 + 2\xi^3 \quad , \quad \phi_4 = -\xi + 2\xi^2 - \xi^3 \tag{3.17}$$

The vector of nodal coordinates in Eq. (2.11) is then

$$\underset{\sim}{w}_j(t) = [w_{j-1}(t) \quad h\theta_{j-1}(t) \quad w_j(t) \quad h\theta_j(t)]^T \ , \ j=1,2,\ldots,N \tag{3.18}$$

where $w_j(t)$ and $\theta_j(t)$ represent translations and rotations, respectively, in which j designates the element number. The nondimensional local coordinate ξ is related to the global coordinate x by $\xi = j - x/h$, as can be concluded from Fig. 3.2.

To obtain the element mass matrices, we insert the interpolation functions given by Eqs. (3.17) into Eq. (2.12a), carry out the integrations and obtain

$$M_j = \int_{(j-1)h}^{jh} m(x)\underset{\sim}{\phi}(x)\underset{\sim}{\phi}^T(x)dx = m_j h \int_0^1 \begin{bmatrix} 3\xi^2 - 2\xi^3 & 3\xi^2 - 2\xi^3 \\ \xi^2 - \xi^3 & \xi^2 - \xi^3 \\ 1 - 3\xi^2 + 2\xi^3 & 1 - 3\xi^2 + 2\xi^3 \\ -\xi + 2\xi^2 - 3\xi^3 & -\xi + 2\xi^2 - \xi^3 \end{bmatrix}^T d\xi$$

$$= \frac{m_j h}{420} \begin{bmatrix} 156 & 22 & 54 & -13 \\ & 4 & 13 & -3 \\ \text{symm} & & 156 & -22 \\ & & & 4 \end{bmatrix} \tag{3.19a}$$

so that

$$\Phi_M = \frac{h}{420}\begin{bmatrix} 156 & 22 & 54 & -13 \\ & 4 & 13 & -3 \\ \text{symm} & & 156 & -22 \\ & & & 4 \end{bmatrix} \tag{3.19b}$$

Similarly, inserting Eqs. (3.17) into Eq. (2.12c) and considering Eq. (3.16), the element stiffness matrices are

$$K_j = \int_{(j-1)h}^{jh} EI(x)\,\frac{d^2\underset{\sim}{\phi}(x)}{dx^2}\,\frac{d^2\underset{\sim}{\phi}^T(x)}{dx^2}\,dx = \frac{EI_j}{h^3}\int_0^1 \begin{bmatrix} 6-12\xi \\ 2-6\xi \\ -6+12\xi \\ 4-6\xi \end{bmatrix}\begin{bmatrix} 6-12\xi \\ 2-6\xi \\ -6+12\xi \\ 4-6\xi \end{bmatrix}^T d\xi$$

$$= k_j \begin{bmatrix} 12 & 6 & -12 & 6 \\ & 4 & -6 & 2 \\ \text{symm} & & 12 & -6 \\ & & & 4 \end{bmatrix} \tag{3.20a}$$

so that

$$\Phi_K = \begin{bmatrix} 12 & 6 & -12 & 6 \\ & 4 & -6 & 2 \\ \text{symm} & & 12 & -6 \\ & & & 4 \end{bmatrix} \tag{3.20b}$$

Note that the stiffness k_j is related to the flexural rigidity of element j according to $k_j = EI_j/h^3$.

As an illustration, we identify a model possessing 15 finite elements, N = 15. The model has 16 nodes and the global mass and stiffness matrices are 32×32. Hence, n = 32 in Eq. (3.14). There are 30 parameters p_i (i=1,2,...,30) to be identified. The parameters are the unknown mass and stiffness average values m_j and k_j (j=1,2,...,15) associated with each element. The structural properties of the beam are illustrated in Fig. 3.1.

To construct the matrix A(t), we turn to Eqs. (3.9a) and (3.9c). The matrix is 32×30 and it is not feasible to give it in full, so that we list only the first two and last two columns. From Eqs. (3.9a), (3.9c), (3.18), (3.19b) and (3.20b), we can write

$$\underset{\sim}{a}_1(t) = \frac{h}{420}\begin{bmatrix} 156\ddot{w}_0(t) + 22h\ddot{\theta}_0(t) + 54\ddot{w}_1(t) - 13h\ddot{\theta}_1(t) \\ 22\ddot{w}_0(t) + 4h\ddot{\theta}_0(t) + 13\ddot{w}_1(t) - 3h\ddot{\theta}_1(t) \\ 54\ddot{w}_0(t) + 13h\ddot{\theta}_0(t) + 156\ddot{w}_1(t) - 22h\ddot{\theta}_1(t) \\ -13\ddot{w}_0(t) - 3h\ddot{\theta}_0(t) - 22\ddot{w}_1(t) + 4h\ddot{\theta}_1(t) \\ 0 \\ \vdots \\ 0 \end{bmatrix} \tag{3.21a}$$

$$\underset{\sim}{a}_2(t) = \frac{h}{420}\begin{bmatrix} 0 \\ 0 \\ 156\ddot{w}_1(t) + 22h\ddot{\theta}_1(t) + 54\ddot{w}_2(t) - 13h\ddot{\theta}_2(t) \\ 22\ddot{w}_1(t) + 4h\ddot{\theta}_1(t) + 13\ddot{w}_2(t) - 3h\ddot{\theta}_2(t) \\ 54\ddot{w}_1(t) + 13h\ddot{\theta}_1(t) + 156\ddot{w}_2(t) - 22h\ddot{\theta}_2(t) \\ -13\ddot{w}_1(t) - 3h\ddot{\theta}_1(t) - 22\ddot{w}_2(t) + 4h\ddot{\theta}_2(t) \\ 0 \\ \vdots \\ 0 \end{bmatrix} \tag{3.21b}$$

$$\underset{\sim}{a}_{29}(t) = \begin{bmatrix} 0 \\ \vdots \\ 0 \\ 12w_{13}(t) + 6h\theta_{13}(t) - 12w_{14}(t) + 6h\theta_{14}(t) \\ 6w_{13}(t) + 4h\theta_{13}(t) - 6w_{14}(t) + 2h\theta_{14}(t) \\ -12w_{13}(t) - 6h\theta_{13}(t) + 12w_{14}(t) - 6h\theta_{14}(t) \\ 6w_{13}(t) + 2h\theta_{13}(t) - 6w_{14}(t) + 4h\theta_{14}(t) \\ 0 \\ 0 \end{bmatrix} \tag{3.21c}$$

$$\underset{\sim}{a}_{30}(t) = \begin{bmatrix} 0 \\ \vdots \\ 0 \\ 12w_{14}(t) + 6h\theta_{14}(t) - 12w_{15}(t) + 6h\theta_{15}(t) \\ 6w_{14}(t) + 4h\theta_{14}(t) - 6w_{15}(t) + 2h\theta_{15}(t) \\ -12w_{14}(t) - 6h\theta_{14}(t) + 12w_{15}(t) - 6h\theta_{15}(t) \\ 6w_{14}(t) + 2h\theta_{14}(t) - 6w_{15}(t) + 4h\theta_{15}(t) \end{bmatrix} \tag{3.21d}$$

To excite at least one elastic mode of the beam, a single transverse forcing function given by

$$f(x,t) = 0.1\ \delta(x - 6h) \cos t \text{ (Newtons)} \tag{3.22}$$

is applied at node 7, where $\delta(x - 6h)$ is a spatial Dirac delta function, so that the rigid-body motions are not significantly excited, although the forcing function has the effect of exciting every mode.

The actual parameters are provided in Table 3.1. The beam has length L = 15 m, so that each discrete element has length h = 1 m. Gaussian random noise is added to the acceleration measurements and the forcing function to the extent that the noise-to-signal ratio is 2% at one standard deviation. The estimated parameters are shown in Tables 3.2 and 3.3 for values of m equal to 4 and 8, respectively, at sampling times t_k = 0.5k (s) (k = 1,2,...,m). Also provided in each table is the normalized root-mean-square (RMS) error. The RMS error is normalized by dividing the error in each parameter by the exact value of the parameter. The results show that increasing the number of sampling instances m in Eq. (3.15) reduces the effect of noise. Table 3.4 shows the actual and computed natural frequencies, as well as the error. The results are excellent.

Conclusions

Space structures can be regarded as distributed-parameter systems characterized by mass, damping and stiffness distributions. A technique for the identification of the mass, damping and stiffness distributions based on the finite element method is presented. The technique has the advantage that it identifies physical properties instead of matrices, which are abstract quantities, not unique for a given structure. The identification process consists of exciting the structure by means of known nodal forces and measuring the response at each nodal degree of freedom. Because the excitation and response are known, the equations of motion can be regarded as a set of simultaneous algebraic equations in the system parameters, and can be solved by a least-squares

technique. The method is stable in the presence of noise. The effect of the noise can be reduced by increasing the number of samplings.

Table 3.1. Mass and Stiffness Distributions of the Free-Free Beam.

Element Number	Mass Distribution	Stiffness Distribution
i	$p_i = m_i$ (kg)	$p_{i+15} = k_i$ (N/m)
1	8.400	3.300
2	1.600	2.300
3	2.300	1.200
4	4.800	1.300
5	6.300	3.300
6	5.200	4.200
7	7.100	1.800
8	4.200	1.400
9	6.300	4.100
10	1.600	3.600
11	1.100	5.200
12	2.400	3.400
13	3.500	6.600
14	4.600	2.500
15	7.300	5.300

Table 3.2. Estimated Parameters for Four Samping Times, $t_k = 0.5k$ (s) (k=1,2,3,4).

Element Number	Mass Distribution	Stiffness Distribution
i	$p_i = m_i$ (kg)	$p_{i+15} = k_i$ (N/m)
1	8.9468	3.4889
2	1.5728	2.3860
3	2.4259	1.2378
4	4.9358	1.3394
5	6.3033	3.3628
6	5.3359	4.2563
7	6.8490	1.7844
8	4.0711	1.3790
9	6.0960	4.0503
10	1.5999	3.5517
11	1.0508	5.1314
12	2.3435	3.3661
13	3.6165	6.5646
14	4.6088	2.4964
15	7.1814	5.3204

RMS Error: 0.056

Table 3.3. Estimated Parameters for Eight Samping Times, $t_k = 0.5k$ (s) (k=1,2,...,8).

Element Number	Mass Distribution	Stiffness Distribution
i	$p_i = m_i$ (kg)	$P_{i+15} = k_i$ (N/m)
1	8.7153	3.3342
2	1.6093	2.3151
3	2.2972	1.2076
4	4.8362	1.3124
5	6.4140	3.3357
6	5.3101	4.2398
7	6.9578	1.7963
8	4.0427	1.3880
9	6.3078	4.1755
10	1.6465	3.6674
11	1.0563	5.2849
12	2.4603	3.4443
13	3.5955	6.6792
14	4.5489	2.5246
15	7.3629	5.3466

RMS Error: 0.035

Table 3.4. First Ten Natural Frequencies of the Free-Free Beam Computed Using the Actual and Estimated Parameters.

r	Actual Natural Frequencies ω_r(rad/s)	Estimated Natural Frequencies ω_r^*(rad/s)	Relative Error $(\omega_r^* - \omega_r)/\omega_r$ (rad/s)
1	0.000000	0.000000	--------
2	0.000000	0.000000	--------
3	0.064455	0.064077	-0.005865
4	0.206939	0.207273	0.001614
5	0.408213	0.408697	0.001186
6	0.719599	0.719890	0.004044
7	1.096452	1.100486	0.003679
8	1.524039	1.530416	0.004184
9	1.999755	2.007110	0.003678
10	2.575960	2.583589	0.002962

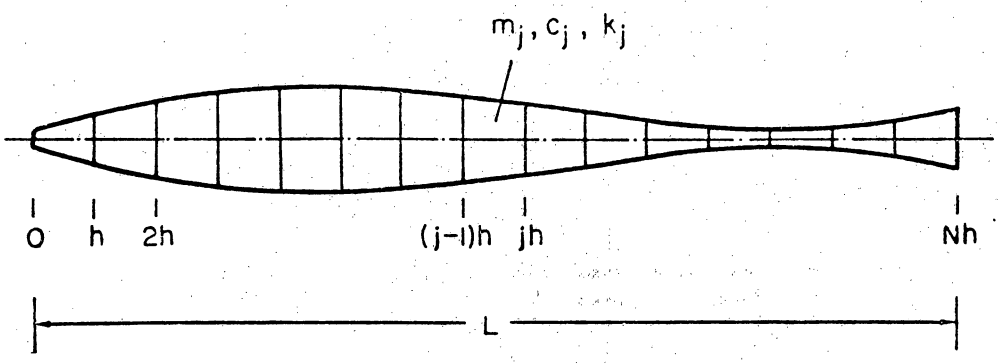

Figure 3.1 The Finite Element Model

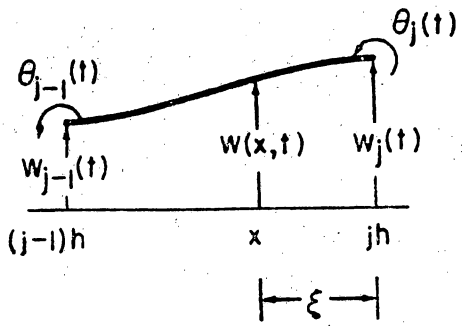

Figure 3.2 A Typical Finite Element Showing Nodal Displacements

Chapter 4

A PERTURBATION TECHNIQUE FOR PARAMETER IDENTIFICATION

In many cases, there is only a preliminary knowledge of the mass, damping and stiffness distributions, and the object is to use this preliminary information to identify the actual distributions. This chapter is conerned with such a case. The preliminary information is used to derive a "postulated" model, which is used as a basis for producing the actual model. Because exact identification of a general distributed system is not possible, the object is to identify approximate mass, damping and stiffness distributions, in the same finite element sense as in Chapter 3. To this end, a perturbation technique is developed in which the postulated model plays the role of the unperturbed, zero-order system and the actual model represents the perturbed system. The implication is that the perturbation, namely, the difference between the actual model and the postulated model, is not very large. The perturbation approach is carried out on an iterative basis, with the results of a given perturbation analysis being used as the postulated model for the next perturbation cycle.

The most striaghtforward case is the one in which measurements of all the nodal displacements are available. In practice, this may be not be realizable. This chapter develops an identification algorithm working with a reduced number of sensor measurements, in which the unknown nodal displacements are treated as pseudo-parameters. One can compute the pseudo-parameters by using the first-order perturbation solution as well as the zero-order solution. In this dissertation we consider only the former. Convergence of the identification process

depends not only on the difference between the actual model and the postulated model but also on the number of sensors used, with the best results being obtained when the full complement of sensor measurements is available.

Chapter 3 presented the identification technique in the time domain. However, as shown in this chapter, the identification technique may also use measurements in the frequency domain. Referring to the finite element equations of motion developed in Chapter 2, the frequency response is derived. Then, the perturbation technique for parameter identification technique including unknown measurements is developed. Finally, the approach is demonstrated by means of a numerical example in which the mass and stiffness distributions of a nonuniform cantilever beam are identified. The example includes sensor and actuator noise.

The Frequency Response

The identification process is carried out in the frequency domain. The first step is to excite the system at different frequencies and measure the frequency response. To this end, we let the excitation have the form

$$\underset{\sim}{F}(t) = \underset{\sim}{F}^{e} e^{i\omega_e t}, \quad e = 1,2,\ldots,m \tag{4.1}$$

where $\underset{\sim}{F}^{e}$ is the amplitude and ω_e the frequency of excitation. Inserting Eq. (4.1) into Eq. (2.13) and dividing the result by $\exp(i\omega_e t)$, we obtain the frequency responses

$$(-\omega_e^2 M + i\omega_e C + K)\underset{\sim}{w}^{e} = \underset{\sim}{F}^{e}, \quad e = 1,2,\ldots,m \tag{4.2}$$

where $i = \sqrt{-1}$.

A Perturbation Technique for Parameter Identification

The proposed identification process is based on the assumption that there is some a priori approximate knowledge of the system parameters and the object is to identify the actual parameters. We refer to the approximate model as "postulated," so that the object is to develop an identification scheme for the actual parameters based on the postulated parameters. Assuming that the difference between the two sets of parameters is small, we consider a perturbation technique in which the postulated parameters represent the unperturbed zero-order solution and the actual parameters represent the perturbed solution, with the difference between the two sets of parameters playing the role of a perturbation.

The postulated parameters corresponding to the finite element model are denoted by m_{0j}, c_{0j} and k_{0j} ($j = 1,2,\ldots,N$), leading to the postulated mass, damping and stiffness matrices M_0, C_0 and K_0, respectively. The corresponding actual parameters and associated matrices are m_j, c_j and k_j and M, C and K, respectively. According to the perturbation scheme, we write

$$m_j = m_{0j} + \Delta m_j, \quad c_j = c_{0j} + \Delta c_j, \quad k_j = k_{0j} + \Delta k_j, \quad j = 1,2,\ldots,N \tag{4.3a,b,c}$$

and

$$M = M_0 + \Delta M, \; C = C_0 + \Delta C, \; K = K_0 + \Delta K \tag{4.4a,b,c}$$

where the increments Δm_j, $\Delta c_j,\ldots,\Delta K$ are small. The identification reduces to the identification of the parameter increments Δm_j, Δc_j and Δk_j ($j = 1,2,\ldots,N$). The procedure is carried out iteratively, in the sense that the results of the first identification cycle will not be regarded as the actual parameters but as improved postulated parameters.

Only when convergence is achieved will the improved postulated parameters be regarded as the actual parameters.

Beginning with the initially postulated parameters m_{0j}, c_{0j} and k_{0j} ($j = 1,2,\ldots,N$), we first compute the matrices M_0, C_0 and K_0 by means of Eqs. (2.12). Then, using Eqs. (4.2), we compute the response vectors $\underset{\sim}{w}_0^e$ ($e = 1,2,\ldots,m$) from the frequency responses

$$[-(\omega^e)^2 M_0 + i\omega^e C_0 + K_0]\underset{\sim}{w}_0^e = \underset{\sim}{F}^e, \quad e = 1,2,\ldots,m \tag{4.5}$$

Next, we consider the "perturbed" frequency responses

$$[-(\omega^e)^2(M_0 + \Delta M) + i\omega^e(C_0 + \Delta C) + K_0 + \Delta K](\underset{\sim}{w}_0^e + \Delta\underset{\sim}{w}^e) = \underset{\sim}{F}^e, \quad e = 1,2,\ldots,m \tag{4.6}$$

The zero-order terms cancel out by virtue of Eqs. (4.5). The first-order terms satisfy the equations

$$[-(\omega^e)^2 \Delta M + i\omega^e \Delta C + \Delta K]\underset{\sim}{w}_0^e = \underset{\sim}{c}^e, \quad e = 1,2,\ldots,m \tag{4.7}$$

where

$$\underset{\sim}{c}^e = -[-(\omega^e)^2 M_0 + i\omega^e C_0 + K_0]\Delta\underset{\sim}{w}^e, \quad e = 1,2,\ldots,m \tag{4.8}$$

in which

$$\Delta\underset{\sim}{w}^e = \underset{\sim}{w}^e - \underset{\sim}{w}_0^e, \quad e = 1,2,\ldots,m \tag{4.9}$$

represents the difference between the measured response vectors $\underset{\sim}{w}^e$ and the corresponding zero-order response vectors $\underset{\sim}{w}_0^e$ computed from Eqs. (4.5).

The perturbation in the system parameters are computed by means of Eqs. (4.7). To this end, we consider the explicit relations between the perturbation matrices and the parameter perturbations as follows

$$\Delta M = \sum_{\ell=1}^{N} \frac{\partial M}{\partial p_\ell}\bigg|_{p_j = m_{0j}} \Delta p_\ell \,, \quad \Delta C = \sum_{\ell=N+1}^{2N} \frac{\partial C}{\partial p_\ell}\bigg|_{p_{N+j} = c_{0j}} \Delta p_\ell, \quad \Delta K = \sum_{\ell=2N+1}^{3n} \frac{\partial K}{\partial p_\ell}\bigg|_{p_{2N+j} = k_{0j}} \Delta p_\ell,$$

$$j = 1,2,\ldots,N \tag{4.10a,b,c}$$

where p_r ($r = 1,2,\ldots,3N$) are the system parameters given by Eq. (3.4). Introducing the $n \times 3N$ matrix

$$B^e = [\underset{\sim}{B}^e_1 \quad \underset{\sim}{B}^e_2 \quad \cdots \quad \underset{\sim}{B}^e_{3N}] \tag{4.11}$$

where

$$\underset{\sim}{B}^e_\ell = \begin{cases} [-(\omega^e)^2 \dfrac{\partial M}{\partial p_\ell}\Big|_{p_j = m_{0j}}]\underset{\sim}{w}^e_0, & \ell = 1,2,\ldots,N \\ [i\omega^e \dfrac{\partial C}{\partial p_\ell}\Big|_{p_j = c_{0j}}]\underset{\sim}{w}^e_0, & \ell = N+1, N+2,\ldots,2N \\ [\dfrac{\partial K}{\partial p_\ell}\Big|_{p_j = k_{0j}}]\underset{\sim}{w}^e_0, & \ell = 2N+1, 2N+2,\ldots,3N \end{cases} \tag{4.12}$$

as well as the 3N-vector of parameter corrections

$$\Delta\underset{\sim}{p} = [\Delta p_1 \quad \Delta p_2 \quad \cdots \quad \Delta p_{3N}]^T \tag{4.13}$$

Eqs. (4.7) can be written in the compact form

$$B^e \Delta\underset{\sim}{p} = \underset{\sim}{c}^e, \quad e = 1,2,\ldots,m \tag{4.14}$$

Equations (4.14) can be combined into

$$B\Delta\underset{\sim}{p} = \underset{\sim}{c} \tag{4.15}$$

where

$$B = \begin{bmatrix} B^1 \\ B^2 \\ \vdots \\ B^m \end{bmatrix}, \quad \underset{\sim}{c} = \begin{bmatrix} \underset{\sim}{c}^1 \\ \underset{\sim}{c}^2 \\ \vdots \\ \underset{\sim}{c}^m \end{bmatrix} \tag{4.16}$$

and we note that B is an $n \cdot m \times 3N$ matrix and $\underset{\sim}{c}$ is an $n \cdot m$-vector.

Equation (4.15) forms the basis for the parameter identification algorithm. Because in general $n \cdot m > 3N$, we must obtain the solution of Eq. (4.15) by a least-squares algorithm [43]. The result is

$$\Delta\underset{\sim}{p} = B^+ \underset{\sim}{c} \tag{4.17}$$

where

$$B^{\dagger} = (B^{T}B)^{-1}B^{T} \tag{4.18}$$

is the pseudo-inverse of B. If B has maximum rank 3N, then $B^{T}B$ is guaranteed to be nonsingular.

As pointed out earlier, the algorithm defined by Eq. (4.17) is applied recursively, in the sense that $\Delta\underset{\sim}{p}$ is used to produce improved postulated system parameters. The iteration process converges when $\Delta\underset{\sim}{p}$ reduces to zero.

Unknown Measurements. Pseudo-Parameters

In practice, implementing Eq. (4.17) may not be realizable because it requires measurements of each nodal displacement. It is desirable to reformulate Eq. (4.17) so as to permit the use of a reduced number of measurements. This requires that we extend the vector of unknown parameters to include the unknown measurements. We refer to these unknown measurements as "pseudo-parameters", because we treat them as parameters for computational purposes.

The response $\underset{\sim}{w}^{e}$ of the actual system contains unknown measurements. Hence, from Eq. (4.9), it is evident that the corresponding components of the perturbation vector $\Delta\underset{\sim}{w}^{e}$ are unknown. We consider the case in which $r < n$ measurements are unknown and split Eq. (4.8) into known and unknown quantities as follows:

$$\underset{\sim}{c}^{e} = -\left[-(\omega^{e})^{2}M_{0} + i\omega^{e}C_{0} + K_{0}\right]I_{n-r}\Delta\underset{\sim n-r}{w}^{e}$$

$$-\left[-(\omega^{e})^{2}M_{0} + i\omega^{e}C_{0} + K_{0}\right]I_{r}\underset{\sim r}{w}^{e} = D^{e}\Delta\underset{\sim n-r}{w}^{e} + E^{e}\Delta\underset{\sim r}{w}^{e} \tag{4.19}$$

where I_{n-r} and I_{r} are $n\times(n-r)$ and $n\times r$-dimensional pseudo-identity matrices, respectively, denoting the positions of known and unknown

measurements, and

$$D^e = - [- (\omega^e)^2 M_0 + i\omega^e C_0 + K_0] I_{n-r} \tag{4.20a}$$

and

$$E^e = - [- (\omega^e)^2 M_0 + i\omega^e C_0 + K_0] I_r \tag{4.20b}$$

are $n\times(n - r)$ and $n\times r$-dimensional coefficient matrices, respectively. The vectors $\Delta\underset{\sim}{w}^e_{n-r}$ and $\Delta\underset{\sim}{w}^e_r$ contain the known and unknown perturbations in the responses, respectively. Hence, reformulating Eqs. (4.14), we have

$$A^e \begin{bmatrix} \Delta\underset{\sim}{p} \\ \hline \Delta\underset{\sim}{w}^e_r \end{bmatrix} = \underset{\sim}{d}^e, \quad e = 1,2,\ldots,m \tag{4.21}$$

where A^e is an $n\times(3N + r)$ matrix given by

$$A^e = [B^e \vdots E^e] \tag{4.22a}$$

and $\underset{\sim}{d}^e$ is an n-dimensional vector given by

$$\underset{\sim}{d}^e = D^e \Delta\underset{\sim}{w}^e_{n-r} \tag{4.22b}$$

Note that a new vector of pseudo-parameters $\Delta\underset{\sim}{w}^e_{n-r}$ $(e = 1,2,\ldots,m)$ is generated at each sampling frequency ω_e $(e = 1,2,\ldots,m)$. To extract the system parameter corrections from Eq. (4.21), we consider m different harmonic excitations ω_e and write

$$A = \begin{bmatrix} B^1 & E^1 & 0 & 0 & \ldots & 0 \\ B^2 & 0 & E^2 & 0 & \ldots & 0 \\ \vdots & \vdots & \vdots & \vdots & & \vdots \\ B^m & 0 & 0 & 0 & \ldots & E^m \end{bmatrix}, \quad \underset{\sim}{d} = \begin{bmatrix} \underset{\sim}{d}^1 \\ \underset{\sim}{d}^2 \\ \vdots \\ \underset{\sim}{d}^m \end{bmatrix} \tag{4.23}$$

where A is an $n\cdot m\times(3N + r\cdot m)$ matrix and $\underset{\sim}{d}$ is an $n\cdot m$-dimensional vector, so that Eqs. (4.21) can be combined into

$$A\Delta\underset{\sim}{p}^* = \underset{\sim}{d} \tag{4.24}$$

where

$$\Delta\underset{\sim}{p}^* = [\Delta\underset{\sim}{p}^T \vdots (\Delta\underset{\sim}{w}_r^1)^T \vdots (\Delta\underset{\sim}{w}_r^2)^T \ \ldots \ (\Delta\underset{\sim}{w}_r^m)^T]^T \tag{4.25}$$

The number of sampling frequencies m must satisfy $m \geq 3N/(n - r)$. When the inequality holds, the solution of Eq. (4.24) can be obtained by a least-squares algorithm, or

$$\Delta\underset{\sim}{p}^* = (A^TA)^{-1}A^T\underset{\sim}{d} \tag{4.26}$$

where A^TA is nonsingular when A has maximum rank $3N + r \cdot m$. Hence, with unknown measurements, the identification process consists of using Eq. (4.26) recursively until the postulated parameters converge to the actual parameters.

Numerical Example

To illustrate the procedure, we identify the mass and stiffness distributions of a nonuniform beam undergoing bending vibration. The example considers both the deterministic and stochastic problems. The stochastic problem is examined by adding Gaussian random noise to the sensor measurements and to the amplitude and frequency of the excitation in the "perturbed" frequency response given by Eq. (4.6).

The energy inner product in Eq. (2.12c) for a cantilever beam undergoing bending vibration is given by Eq. (3.16). The vector of nodal coordinates in Eq. (2.11) is given by Eq. (3.18). The element mass and stiffness matrices are obtained as in the numerical example presented at the end of Chapter 3 and are given by Eqs. (3.19a) and (3.20a), respectively. For this example, we consider a model possessing 6 finite elements, N = 6. The model has 6 nodes and n = 12 degrees of freedom. The system has no damping, so that 12 parameters p_i (i =

1,2,...,12) are to be identified. The parameters are the unknown mass and stiffness distributions m_j and k_j ($j = 1,2,...,6$). The structural properties of the beam are illustrated in Fig. 4.1. Note that the global mass and stiffness matrices are obtained from Eq. (2.14) by crossing out the first two rows and columns corresponding to zero displacement and slope at the clamped end [50].

For the deterministic problem, we consider two cases. In the first case all the measurements are known ($r = 0$) while in the second only one sensor measuring transverse displacement is available ($r = 11$). With no damping, the number of sampling frequencies must satisfy $m \geq 2N/(n-r)$. Hence, in Case 1 we choose $m = 1$ while in Case 2 we chose $m = 12$. The beam is excited harmonically by an actuator applying a transverse load at the free end.

The actual and postulated parameters are provided in Table 4.1. The $m = 12$ sampling frequencies range from 0.5 to 6.0 rad/s in increments of 0.5 rad/s. Case 1 uses the first test frequency only. The beam has length $L = 6$ m, so that each finite element has length $h = 1$ m. Figures 4.2 and 4.3 plot the normalized root-mean-square (RMS) error for each case. The RMS error is normalized by dividing the error in each parameter by the actual value of the parameter. The results indicate that having access to all measurements is less sensitive to perturbations in the parameters. Indeed, Figs. 4.2 and 4.3 show that when all the nodal displacements are measured the permissible initial RMS error is 12% and when only one nodal displacement is measured the - permissible initial RMS error drops to 3%. Note that the RMS error in both cases reduces to zero, so that the postulated parameters converge

to the actual parameters shown in Table 4.1. The convergence is achieved in five iteration steps.

We consider two cases for the stochastic problem using the same analytical set-up as in the deterministic problem. In both cases, Gaussian random noise is added to the sensor measurements and to the excitation of the "perturbed" frequency response. The noise-to-signal ratios in the sensor measurements was 1% and 0.01% for Cases 1 and 2, respectively. The amplitude and frequency of the excitation had noise-to-signal ratios of 0.5% and 0.0005% for Cases 1 and 2 respectively. Figures 4.4 and 4.5 plot the normalized RMS error for each case. The results indicate that the noise disturbs convergence, where Case 2 is highly sensitive to the noise. However, the parameters are improved for both cases.

Conclusions

Structures can be regarded as distributed-parameter systems characterized by mass, damping and stiffness distributions. A perturbation technique converging to the actual parameter distributions of the structure iteratively is presented. The technique is based on the finite element method and does not require a complete set of measurements. Indeed, for the example presented, only a single actuator and sensor were required for the postulated parameters to converge to the actual parameters. The technique has the advantage that it identifies actual parameter distributions, such as mass, damping and stiffness characteristics of elements, rather than entries in mass, damping and stiffness matrices. Note that these entries are abstract quantities and

they are not unique, as they depend on the discretization process and on the number of admissible functions used.

Table 4.1

Actual and Postulated Parameters for Cases 1 and 2

Actual Parameters	Case 1	Case 2
m_1 (kg)	0.92	0.8990
m_2 (kg)	1.28	1.0520
m_3 (kg)	1.17	1.1490
m_4 (kg)	0.63	0.4520
m_5 (kg)	1.11	1.0040
m_6 (kg)	0.98	0.9010
k_1 (N/m)	1.38	1.0420
k_2 (N/m)	0.68	0.7480
k_3 (N/m)	1.24	1.1980
k_4 (N/m)	0.56	0.5520
k_5 (N/m)	0.76	1.1010
k_6 (N/m)	1.12	0.9010

Postulated Parameters	Case 1	Case 2
m_{0_1} (kg)	0.90	0.8600
m_{0_2} (kg)	1.15	1.0100
m_{0_3} (kg)	1.20	1.1300
m_{0_4} (kg)	0.50	0.4400
m_{0_5} (kg)	1.20	0.9800
m_{0_6} (kg)	0.90	0.9000
k_{0_1} (N/m)	1.30	1.0000
k_{0_2} (N/m)	0.60	0.7100
k_{0_3} (N/m)	1.10	1.1700
k_{0_4} (N/m)	0.50	0.5400
k_{0_5} (N/m)	0.90	1.0800
k_{0_6} (N/m)	1.20	0.9000

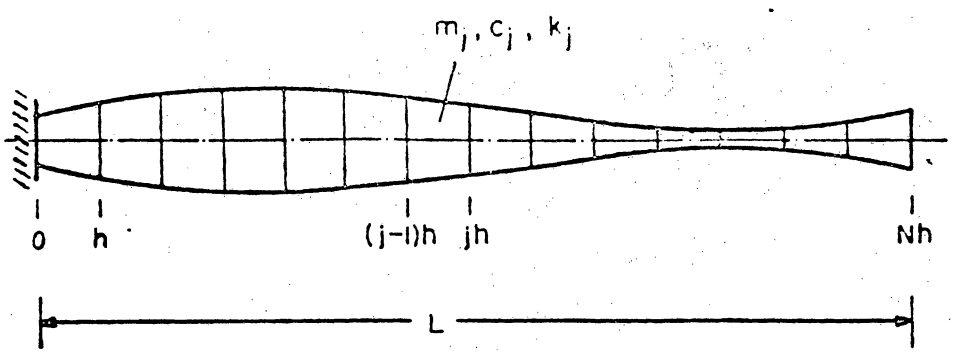

Figure 4.1 Finite Element Model of a Structure

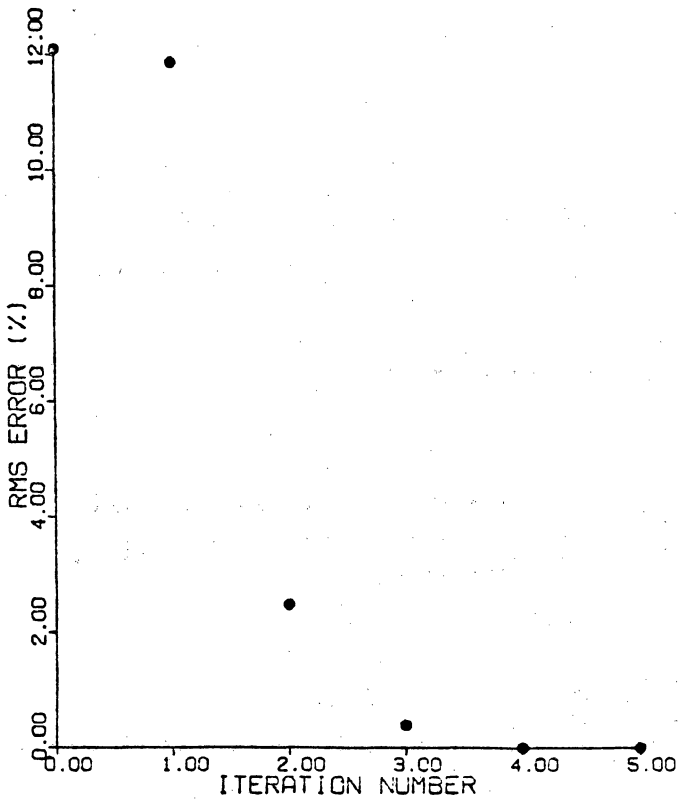

Figure 4.2 Normalized Root-Mean-Square Error for the Case of All Nodal Measurements Given (Deterministic Problem)

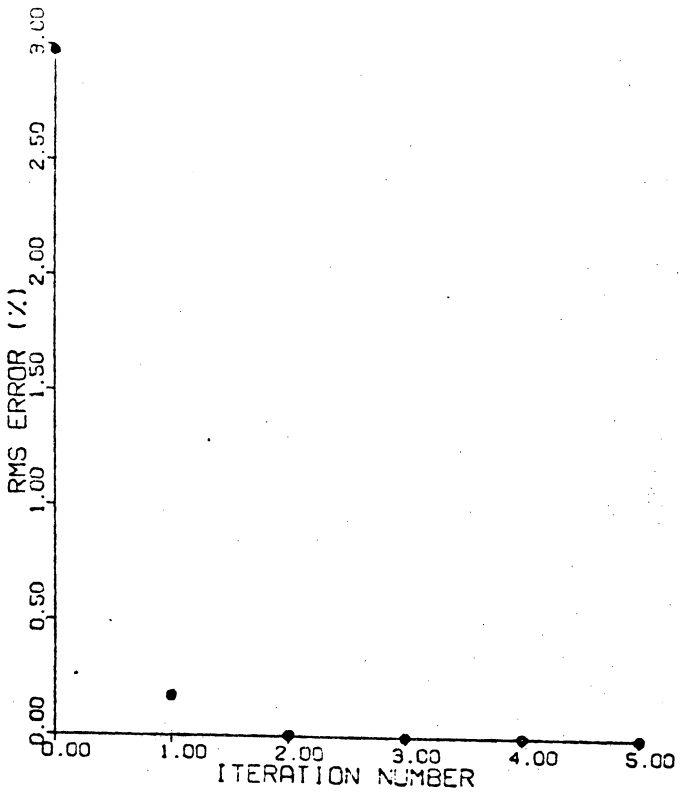

Figure 4.3 Normalized Root-Mean-Square Error for the Case of a Single Nodal Measurement Given (Deterministic Problem).

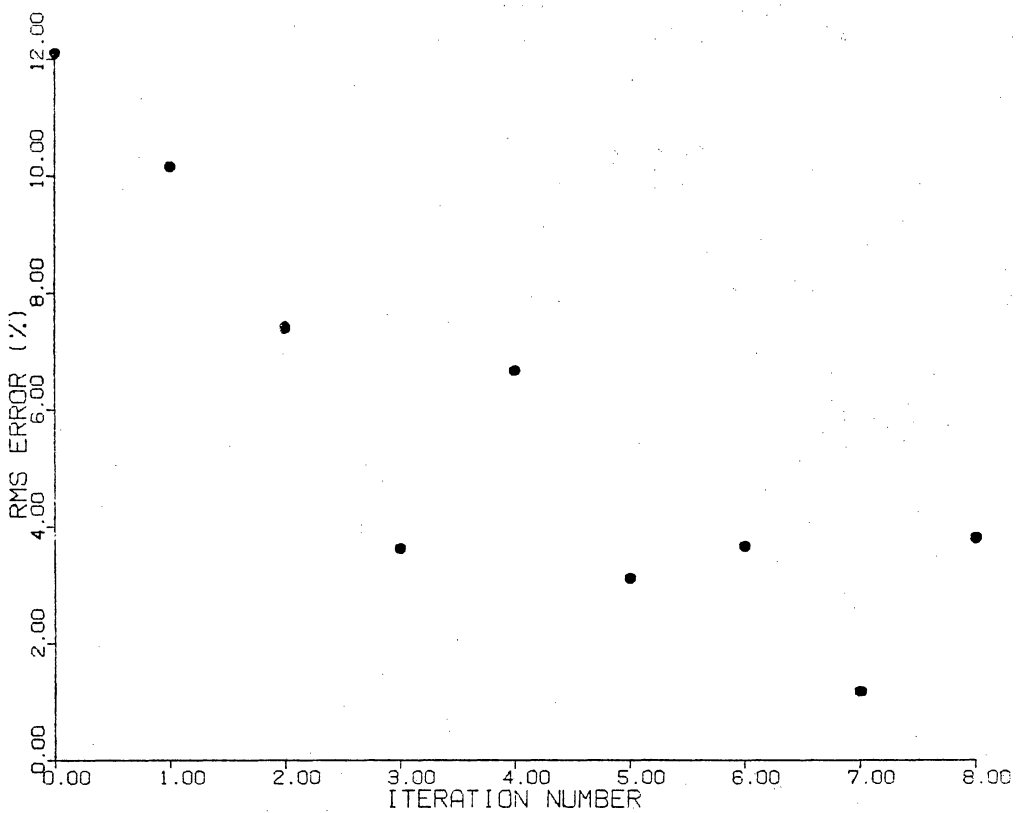

Figure 4.4 Normalized Root-Mean-Square Error for the Case of All Nodal Measurements Given (Stochastic Problem).

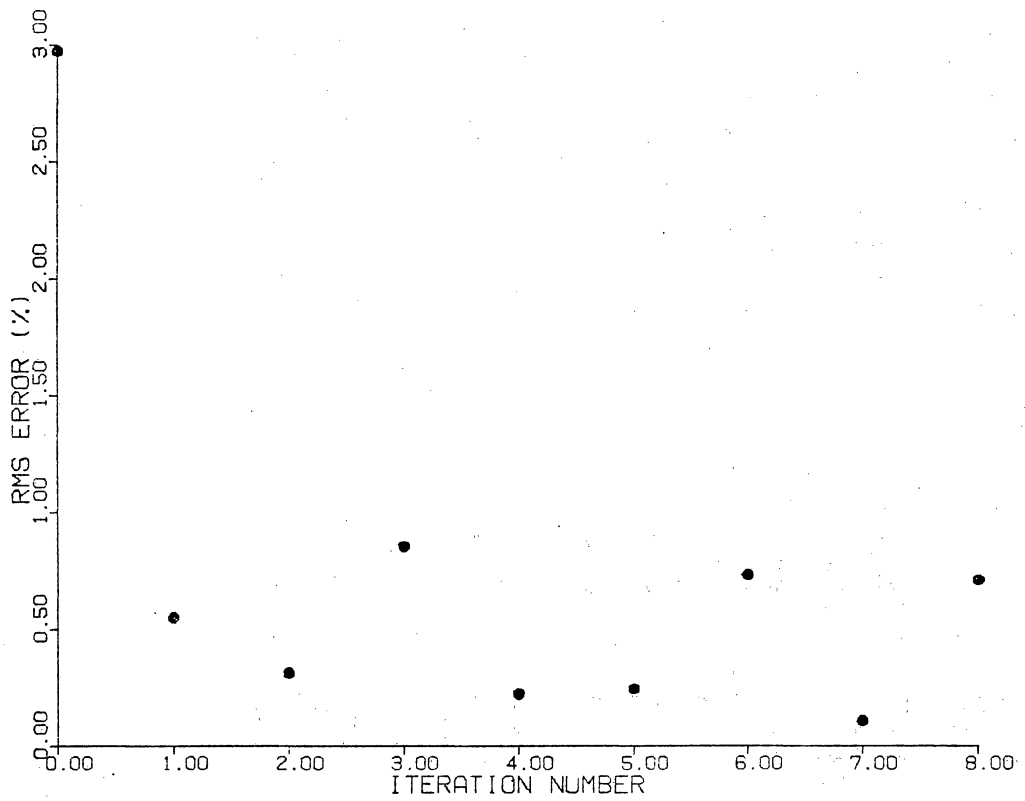

Figure 4.5 Normalized Root-Mean-Square Error for the Case of a Single Nodal Measurement Given (Stochastic Problem).

Chapter 5

MODAL IDENTIFICATION OF SELF-ADJOINT DISTRIBUTED-PARAMETER SYSTEMS

In this chapter, a new method is introduced in which the modal parameters of self-adjoint distributed-parameter systems are identified in the time domain. The method is based on a variational principle, namely Rayleigh's principle, which is applicable to self-adjoint DPS. The technique can be applied to both discrete and continuous systems.

It is common practice to represent the motion of a DPS by a linear combination of the associated modes of vibration. In the case of a DPS, we have an infinite set of modes although, in practice, we are concerned with a finite linear combination of the modes. These modes of vibration possess certain properties which can be used to distinguish them from one another. Indeed, the modes of vibration are uncorrelated in time and orthogonal in space. Frequency-domain methods do not use the spatial orthogonality properties to identify the modes of vibration and encounter problems when the natural frequencies of vibration are closely-spaced or repeated [5,8]. The modal identification method introduced in this chapter uses both the temporal and spatial properties. Because both the temporal and spatial properties are used, the method does not encounter problems when the natural frequencies are closely-spaced or repeated.

Variational Formulation of the Eigenvalue Problem

The eigenvalue problem given by Eqs. (2.2) and (2.3) can be replaced by a variational problem consisting of determining the stationary values of the Rayleigh quotient

$$R(\phi(P)) = \frac{[\phi(P), \phi(P)]}{\int_D m(P)\phi^2(P)dD} \tag{5.1}$$

where [,] represents an energy inner product associated with twice the potential energy of the system. The energy inner product is in symmetric form obtained through an integration by parts of $\int v\mathcal{L}w\, dD$ where v(P) and w(P) are comparison functions satisfying all the boundary conditions in Eq. (2.2) [49]. The advantage of the variational formulation (5.1) lies in the choice of test functions $\phi(P)$, which need only be admissible, i.e., they need only satisfy the geometric boundary conditions.

Let us express $\phi(P)$ as a linear combination of the eigenfunctions, i.e.,

$$\phi(P) = \sum_{r=1}^{\infty} c_r \phi_r(P) \tag{5.2}$$

where c_r are undetermined coefficients. Introducing Eq. (5.2) into (5.1) and considering the spatial orthonormality conditions, Eq. (2.4), we obtain

$$R(c_1, c_2, \ldots) = \sum_{r=1}^{\infty} c_r^2 \omega_r^2 \Big/ \sum_{r=1}^{\infty} c_r^2 \tag{5.3}$$

At the stationary values of R, $\delta R = \sum_{r=1}^{\infty} (\partial R/\partial c_r)\delta c_r = 0$, which implies $\partial R/\partial c_r = 0$ [50]. Hence

$$0 = \partial R/\partial c_r = 2c_r \sum_{i=1}^{\infty} (\omega_r^2 - \omega_i^2)c_i^2 \Big/ \Big(\sum_{i=1}^{\infty} c_i^2\Big)^2 \tag{5.4}$$

From Eqs. (5.4) and (5.3), $R = \omega_r^2$ if $c_r \neq 0$ otherwise $c_r = 0$. Thus, we obtain the denumerably infinite set of solutions

$$R^{(s)} = \omega_s^2 \,, \quad c_r^{(s)} = \delta_{rs} \tag{5.5}$$

Indeed, from Eqs. (5.2) and (5.5), stationary values of the Rayleigh quotient are identical to the eigenvalues and occur when $\phi(P)$ are identical to the corresponding eigenfunctions.

Correlation Between the Modes of Vibration

Consider a freely vibrating undamped system, so that $f(P,t) = 0$ and $C = 0$ in Eq. (2.1). Then, Eq. (2.6) reduces to the independent set of homogeneous second-order differential equations

$$\ddot{u}_r(t) = -\omega_r^2 u_r(t), \quad r = 1,2,... \tag{5.6}$$

Because Eqs. (5.6) are independent, distinct modes of vibration are uncorrelated, so that we can write

$$\langle u_r(t), u_s(t) \rangle = \lim_{T\to\infty} \frac{1}{T} \int_0^T u_r(t) u_s(t) dt = Q_r \delta_{rs}, \quad r,s = 1,2,... \tag{5.7}$$

where the symbol $\langle\ ,\ \rangle$ represents a temporal inner product between the functions $u_r(t)$ $(r = 1,2,...)$ and Q_r $(r = 1,2,...)$ are positive constants. Introducing the solution of Eq. (5.6) into (5.7), it can be shown that

$$\lim_{T\to\infty} \frac{1}{T} \langle \dot{u}_r(t), \dot{u}_s(t) \rangle = \omega_r^2 Q_r \delta_{rs}, \quad r,s = 1,2,... \tag{5.8}$$

and

$$\lim_{T\to\infty} \frac{1}{T} \langle \ddot{u}_r(t), u_s(t) \rangle = \omega_r^2 Q_r \delta_{rs}, \quad r,s = 1,2,... \tag{5.9}$$

Modal Identification for Self-Adjoint Distributed-Parameter Systems

Our objective is to identify the eigenvalues λ_r and the corresponding eigenfunctions $\phi_r(P)$ from the free response. To that end, we define another a pseudo-Rayleigh quotient suitable for modal identification. The Rayleigh quotient is given by

$$R(\xi(P)) \lim_{T\to\infty} \frac{1}{T} = \langle \ddot{u}(t), u(t) \rangle \Big/ \lim_{T\to\infty} \frac{1}{T} \langle u(t), u(t) \rangle \tag{5.10}$$

where

$$u(t) = \int_D \xi(P) u(P,t) dD \tag{5.11}$$

in which $\xi(P)$ are functions satisfying the geometric boundary conditions, Eq. (2.2). We can express the admissible function $\xi(P)$ as

$$\xi(P) = \sum_{r=1}^{\infty} a_r m(P) \phi_r(P) \tag{5.12}$$

Introducing Eq. (5.12) into (5.11) and the result into (5.10), considering the spatial orthonormality conditions, Eq. (2.4), the correlation properties, Eq. (5.7), and the equations of motion, Eq. (5.6), we obtain

$$R(a_1, a_2 \ldots) = \sum_{r=1}^{\infty} \omega_r^2 a_r^2 Q_r \Big/ \sum_{r=1}^{\infty} a_r^2 Q_r \tag{5.13}$$

At the stationary values of R, we have [50]

$$0 = \partial R / \partial a_r = 2a_r \sum_{i=1}^{\infty} (\omega_r^2 Q_r - \omega_i^2 Q_i) a_i^2 \Big/ \left(\sum_{i=1}^{\infty} a_i^2 \right)^2 \tag{5.14}$$

From Eqs. (5.4) and (5.14), $R = \omega_r^2$ if $a_r \neq 0$, otherwise $a_r = 0$. We obtain the denumerably infinite set of solutions

$$R^{(s)} = \omega_s^2, \quad a_r^{(s)} = \delta_{rs}, \quad r,s = 1,2,\ldots \tag{5.15}$$

Indeed, from Eqs. (5.13) and (5.15), stationary values of the Rayleigh quotient, Eq. (5.10), are identical to the eigenvalues and they occur when $\xi(P)$ is equal to the corresponding eigenfunctions multiplied by the mass distribution.

Equation (5.11) implies that distributed measurements are required in order to form the Rayleigh quotient, Eq. (5.10). However, it is often impractical to measure $u(P,t)$ completely. Therefore, one resorts to approximate methods.

Approximate Methods

We can express both the functions $\xi(P)$ and the displacement $u(P,t)$ as linear combinations of the admissible functions $\psi_r(P)$, as

$$\xi^{(n)}(P) = \sum_{r=1}^{n} v_r \psi_r(P), \quad u^{(n)}(P,t) = \sum_{r=1}^{n} w_r(t)\psi_r(P) \tag{5.16}$$

where $\xi^{(n)}(P)$ is the nth order approximation of $\xi(P)$, $u^{(n)}(P,t)$ is the nth order approximation of $u(P,t)$ and where v_r and $w_r(t)$ are undetermined coefficients. Introducing Eqs. (5.16) into (5.11), we obtain

$$u(t) = \sum_{r=1}^{n} \sum_{s=1}^{n} v_r w_s(t)\psi_{rs}, \quad \psi_{rs} = \int_D \psi_r(P)\psi_s(P)dD \tag{5.17}$$

Introducing Eqs. (5.17) into (5.10), we obtain

$$R(v_1,v_2\ldots,v_n) = \sum_{r=1}^{n} \sum_{s=1}^{n} b_{rs}^{(n)} v_r v_s \Big/ \sum_{r=1}^{n} \sum_{s=1}^{n} a_{rs}^{(n)} v_r v_s \tag{5.18}$$

where

$$a_{rs}^{(n)} = a_{sr}^{(n)} = \sum_{i=1}^{n} \sum_{j=1}^{n} \psi_{ri}\,\psi_{sj} \lim_{T\to\infty} \frac{1}{T} \langle w_i(t), w_j(t)\rangle, \tag{5.19}$$

$$b_{rs}^{(n)} = b_{sr}^{(n)} = \sum_{i=1}^{n} \sum_{j=1}^{n} \psi_{ri}\psi_{sj} \lim_{T\to\infty} \frac{1}{T} \langle \ddot{w}_i(t), w_j(t)\rangle \tag{5.20}$$

Now, determining the stationary values of the Rayleigh quotient, Eq. (5.18) can be replaced by the eigenvalue problem

$$\lambda^{(n)} A^{(n)} \underset{\sim}{v}^{(n)} = B^{(n)} \underset{\sim}{v}^{(n)} \tag{5.21}$$

where Eq. (5.21) represents the nth-order approximation of Eq. (5.10), and where $A^{(n)}$, $B^{(n)}$ and $\underset{\sim}{v}^{(n)}$ have entries $a_{rs}^{(n)}$, $b_{rs}^{(n)}$ and $v_r^{(n)}$, respectively. From Eqs. (5.18), (5.19) and (5.20)

$$A^{(n)} = \psi^{(n)} A_o^{(n)} \psi^{(n)}, \quad B^{(n)} = \psi^{(n)} B_o^{(n)} \psi^{(n)} \tag{5.22}$$

where $\psi^{(n)}$, $A_o^{(n)}$ and $B_o^{(n)}$ are n×n matrices with entries ψ_{rs}, a_{ors} and b_{ors}, respectively, in which

$$a_{ors} = a_{osr} = \lim_{T\to\infty} \frac{1}{T} \langle w_r(t), w_s(t) \rangle, \quad b_{ors} = b_{osr} = \lim_{T\to\infty} \frac{1}{T} \langle \ddot{w}_r(t), w_s(t) \rangle \tag{5.23}$$

Finally, the eigenvalue problem, Eq. (5.21), can be simplified if we consider the change of variables

$$\underset{\sim}{w}^{(n)} = \psi^{(n)} \underset{\sim}{v}^{(n)} \tag{5.24}$$

Introducing Eq. (5.24) into (5.21) and premultiplying the result by $\psi^{-(n)}$, we obtain the eigenvalue problem in the form

$$\lambda^{(n)} A_o^{(n)} \underset{\sim}{w}^{(n)} = B_o^{(n)} \underset{\sim}{w}^{(n)} \tag{5.25}$$

The question still remains how to obtain $w_r(t)$ and $\dot{w}_r(t)$ in Eqs. (5.19) and (5.20) from the system response. Indeed, the answer depends on the nature of the admissible functions.

Perhaps the most popular type of approximation is the finite element approximation in which one considers admissible functions as interpolation functions. Using a finite element approximation, $w_r(t)$ become measurements taken at nodal points and, using the interpolation functions $\psi_r(P)$, a distributed profile for $u(P,t)$ is obtained.

The Collocation Approximation [50]

Let us measure displacements and velocities at points P_r ($r = 1,2,\ldots,n$) in the domain D. Then, the function $\xi(P)$ is approximated by

$$\xi(P) \cong \sum_{r=1}^{n} \xi^{(n)}(P)\, \delta(P - P_r) \tag{5.26}$$

where $\xi^{(n)}(P_r)$ represents the nth-order approximation of $\xi(P_r)$. Introducing Eq. (5.26) into (5.11), we obtain

$$u(t) = \sum_{r=1}^{n} \xi^{(n)}(P_r)u(P_r,t) = \sum_{r=1}^{n} v_r\, u(P_r,t) \tag{5.27}$$

where $v_r = \xi^{(n)}(P_r)$. Introducing Eq. (5.27) into (5.10), yields

$$R(v_1,v_2,\ldots,v_n) = \sum_{r=1}^{n}\sum_{s=1}^{n} v_r v_s\, b_{rs}^{(n)} \Big/ \sum_{r=1}^{n}\sum_{s=1}^{n} v_r v_s a_{rs}^{(n)} \tag{5.28}$$

in which

$$a_{rs}^{(n)} = a_{sr}^{(n)} = \lim_{T\to\infty} \frac{1}{T} \langle u(P_r,t),\, u(P_s,t)\rangle,\quad b_{rs}^{(n)} = b_{sr}^{(n)}$$

$$= \lim_{T\to\infty} \frac{1}{T} \langle \ddot{u}(P_r,t),\, u(P_s,t)\rangle \tag{5.29}$$

Now, determining the stationary values of the Rayleigh quotient, Eq. (5.28), is equivalent to solving the eigenvalue problem [50]

$$\lambda^{(n)}\, A^{(n)}\, \underset{\sim}{v}^{(n)} = B^{(n)}\, \underset{\sim}{v}^{(n)} \tag{5.30}$$

where $A^{(n)}$, $B^{(n)}$ and $\underset{\sim}{v}^{(n)}$ have entries $a_{rs}^{(n)}$, $b_{rs}^{(n)}$ and $v_r^{(n)}$, respectively.

Numerical Examples

To illustrate the identification process, we consider two examples. In the first example, the modal parameters associated with the bending vibration of a uniform simply-supported beam are identified. In the second example, the modal parameters associated with a finite element model of a uniform square membrane subjected to a constant tension T with all its boundaries free are identified.

The stiffness operator for the beam in bending vibration is given by [49]

$$L = \frac{\partial^2}{\partial x^2}\left[EI(x)\, \frac{\partial^2}{\partial x^2}\right],\quad 0 < x < L \tag{5.31}$$

where EI denotes the flexural rigidity of the beam. For convenience, we choose m = 1 kg/m, EI = 1 $N \cdot m^2$ and L = 10 m. The eigenvalue problem, Eq. (2.3), admits the closed-form solution

$$\lambda_r = \omega_r^2 = \left(\frac{r\pi}{L}\right)^4, \quad \phi_r(P) = \sqrt{\frac{1}{5}} \sin\left(\frac{r\pi x}{L}\right), \quad 0 < x < L, \quad r = 1,2,\ldots \tag{5.32}$$

We wish to identify the ten lowest eigenvalues and corresponding eigenfunctions using ten discrete sensors measuring transverse displacements and velocities at locations equally spaced along the beam. The identification process uses the free response of the beam initially excited by an impulse of magnitude 1 N at x = 10/11 m. Fifteen modes are simulated in the response. Using the collocation approximation, the identification process is completed by solving the eigenvalue problem given by Eq. (5.30). The inner products in Eq. (5.29) are approximated by using T = 100 (sec) in Eq. (5.7) where

$$a_{ors} = \lim_{T\to\infty} \frac{1}{T} \langle u(x_r,t), u(x_s,t)\rangle, \quad b_{ors} = \lim_{T\to\infty} \frac{1}{T} \langle \ddot{u}(x_r,t), u(x_s,t)\rangle \tag{5.33}$$

$$x_r = r\left(\frac{L}{11}\right) \text{ m}, \quad r = 1,2,\ldots,10$$

Table 5.1 lists both the identified and actual natural frequencies together with the percentage errors. Figures 5.1 and 5.2 show the identified eigenvectors together with the normalized eigenfunctions for the first ten modes of vibration. Note that the identified natural frequencies and eigenvectors agree well with the actual natural frequencies and actual normalized mode shapes, respectively. The disagreement is due to the approximation of Eq. (5.7) and the collocation approximation. Because the mass distribution is unity for this case, the identified eigenvectors are identical to the normalized eigenfunc-

tions to within a multiplicative constant. In general, the identified eigenvectors will agree with the actual normalized eigenfunctions only when the mass distribution is known.

As a second illustration, we identify the lowest five natural frequencies associated with a finite element model of a uniform square membrane under constant tension T with all its boundaries free. The stiffness operator for the membrane is given by [50]

$$L = -\frac{\partial}{\partial x}\left(T\frac{\partial}{\partial x}\right) - \frac{\partial}{\partial y}\left(T\frac{\partial}{\partial y}\right) \tag{5.34}$$

As shown in Figure 5.3, the membrane has triangular elements corresponding to 16 nodal degrees of freedom. Using linear interpolation functions as admissible functions yields the natural frequencies given in Table 5.2. Note that some of the natural frequencies in this example are repeated.

In order to identify the five lowest natural frequencies, 16 sensors measuring transverse velocities and accelerations at each node are used. The displacement profile u(P,t) and the admissible functions $\xi(P)$ in Eq. (5.16) are approximated using linear finite element interpolation functions [50]. We choose as admissible functions $\xi(P)$, the eigenfunctions of the uniform membrane subjected to constant tension T and with all its boundaries free [50]. The initial displacements of the membrane were taken as zero. The initial velocities were taken as zero except at node 5 where the membrane was given an initial velocity of 1 m/s. The identification process is completed by determining the solution to Eq. (5.22), where the entries in $A^{(n)}$ and $B^{(n)}$ are given in Eqs. (5.19) and (5.20), respectively, with the exception that the dis-

placements in Eq. (5.19) are replaced by velocities and the velocities in Eq. (5.20) are replaced by accelerations. This is necessary due to the presence of a rigid-body mode of vibration. Indeed, the acceleration and velocity of the rigid-body modes in free motion are uncorrelated in time although the velocity and displacement are not. The temporal correlation properties in Eqs. (5.8) and (5.9) are approximated using T = 100 (sec). The identified natural frequencies and percentage error are given in Table 5.2. The identified eigenvectors are shown in Figure 5.4. As in the beam example, the identified eigenvectors agree well with the normalized eigenvectors of the membrane model.

Conclusions

A new method is introduced for the identification of modal parameters of DPS. The method considers both the temporal correlation and spatial characteristics of self-adjoint DPS, whereby temporal and spatial orthogonality properties form a Rayleigh quotient for the system. The method has been shown to work well for continuous and discrete systems and does not encounter problems with closely-spaced or repeated natural frequencies.

Table 5.1

Actual and Identified Natural Frequencies for the Simple Beam

Actual Natural Frequencies (rad/s)	Identified Natural Frequencies (rad/s)	Percentage Error (o/o)
0.09870	0.09834	0.4
0.39478	0.39433	0.1
0.88826	0.88821	0.0
1.57914	1.57910	0.0
2.46740	2.46734	0.0
3.55306	3.55311	0.0
4.83611	6.68212	-38.2
6.31655	8.49410	-34.5
7.99438	10.19992	-27.6
9.86960	11.46529	-16.2

Table 5.2

Actual and Identified Natural Frequencies for the Free-Free Membrane

Actual Natural Frequencies (rad/s)	Identified Natural Frequencies (rad/s)	Percentage Error (o/o)
0.0000	0.0000	0.0
1.1912	1.1835	0.6
1.1915	1.1948	-0.3
2.7641	2.7669	-0.1
5.8445	5.8482	-0.1
5.8544		
7.8315		
9.4418		
12.0000		
12.0000		
15.3027		
16.0685		
17.8975		
25.1564		
25.6702		
29.5497		

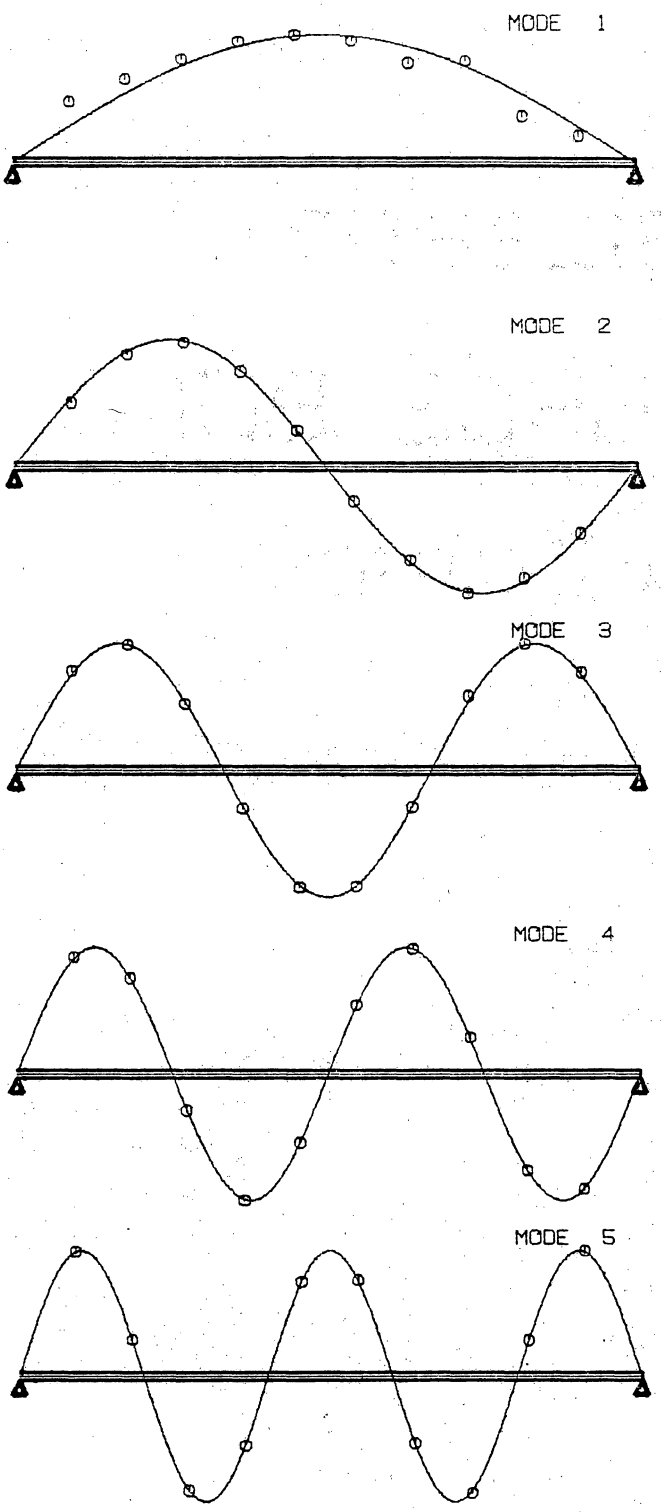

Figure 5.1 Identified and Normalized Eigenvectors for Modes 1 through 5 of the Uniform Simple Beam.

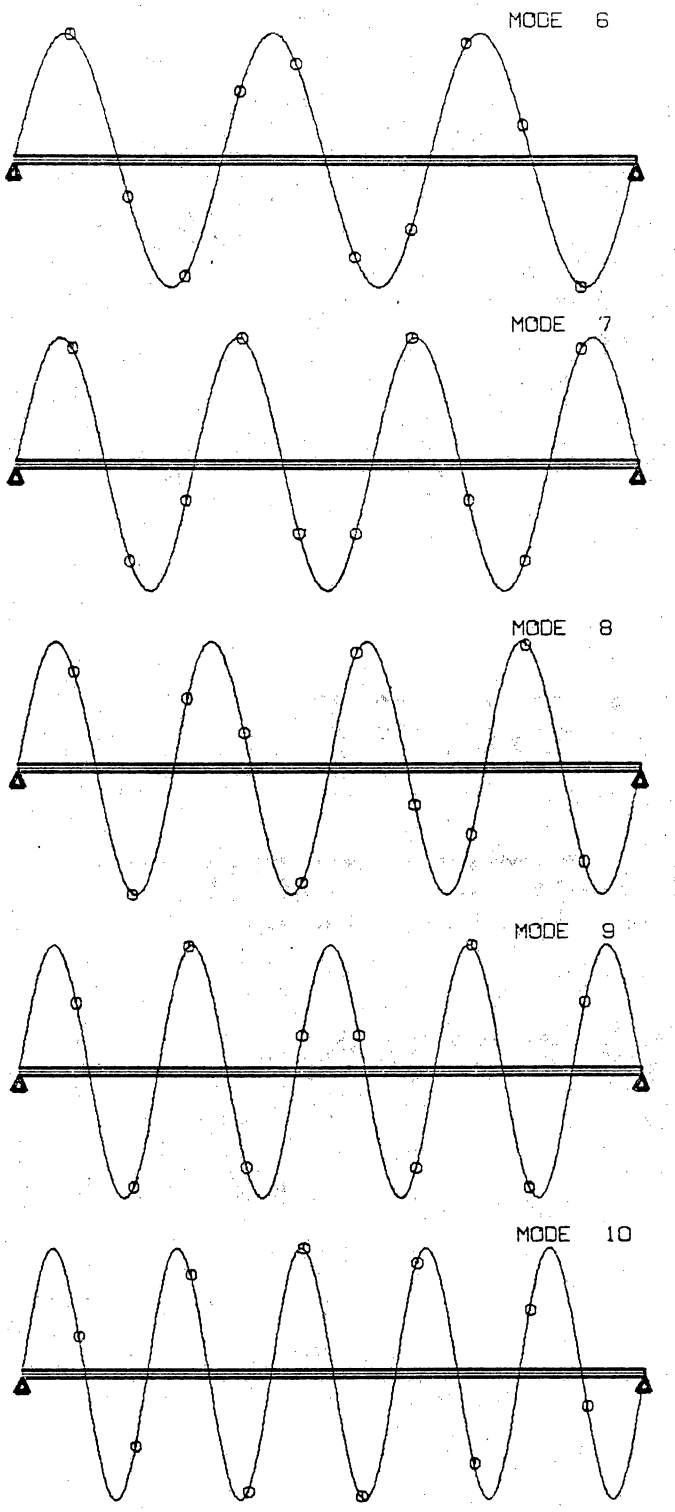

Figure 5.2 Identified and Normalized Eigenvectors for Modes 6 through 10 of the Uniform Simple Beam.

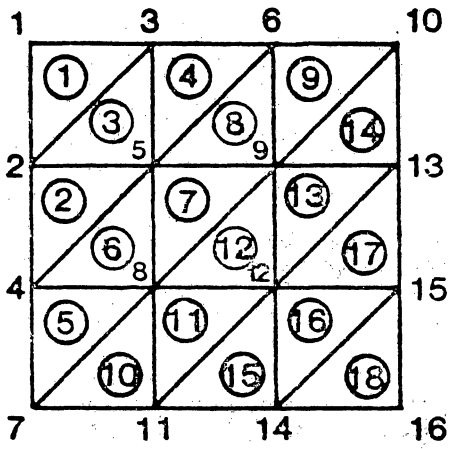

Figure 5.3 Membrane Finite Element Model.

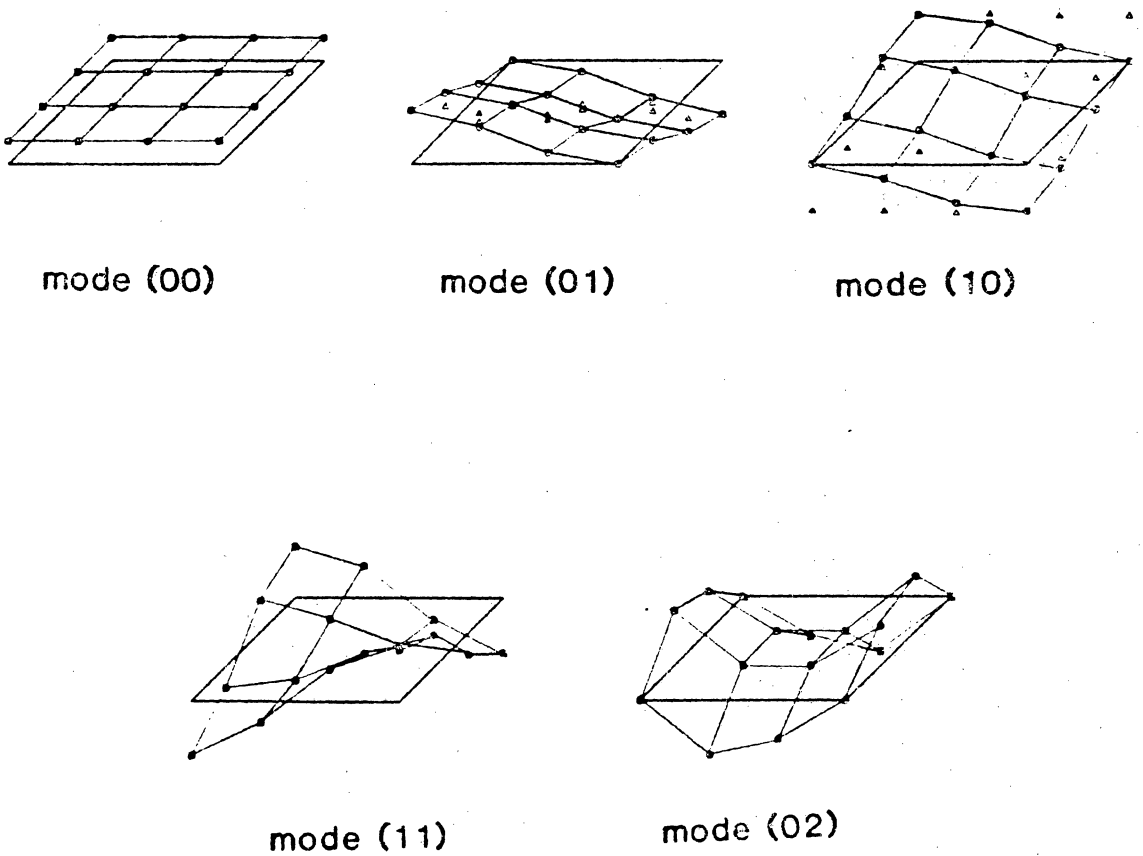

Figure 5.4 Identified and Normalized Eigenvectors of the Uniform Membrane.

REFERENCES

1. Flanelly, W. G. and Berman, A., "The State of the Art of System Identification of Vibrating Structures," System Identification of Vibrating Structures, ASME Publications, New York, 1972, pp. 121-131.

2. Cohen, R., "Identification in Vibratory Systems, A Survey," Proceedings of the 1974 Joint Automatic Control Conference, Austin, Texas, June 17-21, 1974.

3. Kubrusly, C. S., "Distributed Parameter System Identification, A Survey," International Journal of Control, Vol. 26, No. 4, 1977, pp. 509-535.

4. Hart, G. C. and Yao, J. T., "System Identification in Structural Dynamics," Journal of the Engineering Mechanics Division, December 1977, pp. 1089-1104.

5. Berman, A., "Determining Structural Parameters from Dynamic Testing," Shock and Vibration Digest, Vol. 7, No. 1, January 1974, pp. 10-17.

6. Berman, A., and Flanelly, W. G., "Theory of Incomplete Models of Dynamic Structures," AIAA Journal, Vol. 9, No. 8, August 1971, pp. 1481-1487.

7. Raney, J. P. and Howlett, J. T., "Identification of Structural Systems by use of Near Resonance Testing," NASA TN D-5069, 1968.

8. Ewins, D. J., Modal Testing: Theory and Practice, John Wiley & Sons, New York, 1984.

9. Chen, J. C. and Garba, J. A., "Analytical Model Improvement Using Modal Test Results," AIAA Journal, Vol. 18, No. 6, June 1980, pp. 684-690.

10. Hendricks, S. L., Hayes, S. L. and Junkins J. L., "Structural Parameter Identification for Flexible Spacecraft," AIAA Paper No. 84-0060 presented at the 22nd Aerospace Sciences Meeting, Jan. 1984, Reno, Nevada.

11. Meirovitch, L. and Baruh, H., "Identification of Distributed-Parameter Vibrating Systems," 6th IFAC Symposium on Identification and System Parameter Estimation, Washington, D.C., June 7-11, 1982.

12. Berman, A., "Mass Matrix Correction Using an Incomplete Set of Measured Modes," AIAA Journal, Vol. 17, October 1979, pp. 1147-1148.

13. Berman, A., and Nagy, E. J., "Improvement of a Large Analytical Model Using Test Data," AIAA Journal, Vol. 21, August 1983, pp. 1168-1173.

14. Link, M., "Theory of a Method for Identifying Incomplete System Matrices from Vibrating Test Data," Z. Flugwiess Weltraumforsch. Vol. 9, No. 2, 1985, pp. 76-82.

15. Dale, O. B. and Cohen, R., "Multiparameter Identification in Linear Continuous Vibratory Systems," Journal of Dynamic Systems, Measurement and Control, Vol. 93, March 1971, pp 45-52.

16. Spalding, G. R., "Distributed System Identification: A Green's Function Approach," Journal of Dynamic Systems, Measurement and Control, Vol. 98, June 1976, pp. 146-151.

17. Weeks, C., "The Control and Estimation of Large Space Structures," Proceedings of the Joint Automatic Control Conference, Vol. 2, August 13-15, San Francisco, CA, 1980.

18. Juang, J. N. and Sun, C. T., "System Identification of Large Flexible Structure by Using Simple Continuum Models," Journal of Astronautical Sciences, Vol. XXXI, No. 1, Jan.-Mar. 1983, pp. 77-98.

19. Ibrahim, S. R. and Mikulcik, E. C., "The Experimental Determination of Vibration Parameters for Time Responses," Shock and Vibration Bulletin, Vol. 46, Pt. 5, 1976, pp. 187-196.

20. Ibrahim, S. R. and Mikulcik, E. C., "A Method for the Direct Identification of Vibration Parameters from the Free Response," Shock and Vibration Bulletin, Vol. 47, Pt. 4, 1977, pp. 183-198.

21. Ibrahim S. R., "Limitations of Random Input Forces in Randomdec Computation for Modal Identification," Shock and Vibration Bulletin, Vol. 50, Pt. 3, 1980, pp. 99-112.

22. Ibrahim, S. R. and Pappa, R. S., "Large Modal Survey Testing Using the Ibrahim Time Domain (ITD) Identification Technique," Proceedings of the 22nd SDM Conference, Atlanta, GA, April 6-8, 1981, Pt. 2, pp. 173-186.

23. Andrew, L. V., "An Automated Application of Ibrahim's Time Domain Method to Responses of the Space Shuttle, "Proceedings of the 22nd SDM Conference, Atlanta, Georgia, April 6-8, 1981, Pt. 2, pp. 155-165.

24. Baruh, H. and L. Meirovitch, "Identification of the Eigensolution of Distributed-Parameter Systems," AIAA/ASME/ASCE/AHS 23rd SDM Conference, New Orleans, LA, 1982.

25. Sundararajan, N. and Montgomery, R. C., "Identification of Structural Dynamic Systems Using Least-Square Lattice Filters," Journal of Guidance, Control and Dynamics, Vol. 6, No. 5, Sept.-Oct. 1983, pp. 374-381.

26. Juang, J. N. and Pappa, R. S., "An Eigensystem Realization Algorithm for Modal Parameter Identification and Model Reduction," Journal of Guidance, Control, and Dynamics, Vol. 8, No. 6, Sept.-Oct. 1985, pp. 620-627.

27. Pappa, R. S. and Juang, J. N., "Galileo Spacecraft Modal Identification Using an Eigensystem Realization Algorithm," AIAA Dynamics Specialists Conference, Palm Springs, CA, 17-18 May 1984.

28. Ewins, D. J. and Gleeson, P. T., "A Method for Modal Identification of Lightly Damped Structures," Journal of Sound and Vibration, Vol. 31, 1980, pp. 57-79.

29. Jezequel, L., "Three New Methods of Modal Identification," Journal of Vibration, Acoustics, Stress, and Reliability in Design, Trans. ASME, Vol. 108, January 1986, pp. 17-25.

30. Prado, G. and Pearson, R. K., "Efficient Techniques for System Identification of Large Space Structures," Proceedings of the Joint Automatic Control Conference, Vol. 2, August 13-15, San Francisco, CA, 1980.

31. Yedavalli, R. K. and Skelton, R. E., "Determination of Critical Parameters in Large Flexible Space Structures with Uncertain Modal Data," Journal of Dynamic Systems, Measurement and Control, Vol. 105, December 1983, pp. 238-244.

32. Shinozuka, M., Yun, C. B. and Hiroyuki, I., "Identification of Linear Structural Dynamic Systems," Journal of Engineering Mechanics Division, December, 1982, pp. 1371-1390.

33. Wu, Y . W. A., "Guaranteed Error Estimation/Identification and its Applications to Large Flexible Space Structures," Proceedings of the Joint Automatic Control Conference, Vol. 2, August 13-15, San Francisco, CA, 1980.

34. Saridis, G. N., "Comparison of Five Popular Identification Algorithms: A Survey," Proceedings of the 1972 IEEE Conference on Decision and Control, Paper No. WA3-4, 1972, pp. 40-45.

35. Rodriguez, G., "Model Error Estimation for Large Space Structures," Proceedings of the Joint Automatic Control Conference, Vol. 2, August 13-15, San Francisco, CA, 1980.

36. Wells, W. R., "Application of Modern Parameter Estimation Methods to Vibrating Structures," Shock and Vibration Digest, Vol. 47, Part 4, 1977, pp. 155-159.

37. Soderstrom, T., Ljung, L. and Gustavsson, I., "A Theoretical Analysis of Recursive Identification Methods," Automatica, Vol. 14, pp. 231-244, 1978.

38. Leuridan, J. M. and Brown, D. L., "Direct System Parameter Identification of Mechanical Structures with Application to Modal Analysis," Proceedings of the AIAA/ASME/ASCE/AHS 23rd Structures, Structural Dynamics and Materials Conference, May 1982, pp. 548-556.

39. Caravani, P., Watson, M. L. and Thomson, W. T., "Recursive Least-Squares Time Domain Identification of Structural Parameters," Journal of Applied Mechanics, March 1977, pp. 135-140.

40. Hendricks, S. L., Rajaram, S., Kamat, M. P. and Junkins J. L., "Identification of Large Flexible Structures Mass/Stiffness and Damping from On-Orbit Experiments," Journal of Guidance, Control and Dynamicx, Vol. 7, No. 2, March-April 1984, pp. 244-245.

41. Rajaram, S., "Identification of Vibrating Parameters of Flexible Structures," PHD Thesis, VPI&SU, May 1984.

42. Rajaram, S. and Junkins, J. L., "Identification of Vibrating Flexible Structures," Journal of Guidance, Control and Dynamics, Vol. 8, No. 4, July-august 1984, pp. 463-470.

43. Junkins, J. L., Optimal Estimation Methods, Sijthoff & Noordhoff, The Netherlands, 1978.

44. Nayfeh, A. H. and Hefzy, M. S. "Continuum Modeling of Three Dimensional Truss-Like Space Structures," AIAA Journal, Vol. 16, No. 8, 1978, pp. 779-787.

45. Noor, A. K. and Nemeth, M. P., "Analysis of Spatial Beam-Like Lattices with Rigid Joints," Computer Methods in Applied Mechanics and Engineering, Vol. 24, 1980, pp. 35-39.

46. Chen, C. C. and Sun, C. T., "Transient Analysis of Large Frame Structures by Simple Models," Journal of Astronautical Sciences, Vol. 31, No. 3, 1983, pp. 359-379.

47. Sun, C. T. and Juang, J. N., "Modeling Global Structural Damping in Trusses Using Simple Continuum Models," AIAA Journal, Vol. 24, No. 1, 1986, pp. 144-150.

48. Sun, L. T. and Liebbe, S. W., "A Global-Local Approach to Solving Vibration of Large Truss Structures," Proceedings of the AIAA/ASME/ASCE/AHS 27th Structures, Structural Dynamics and Materials Conference, April 1986, pp. 248-255.

49. Meirovitch, L., Analytical Methods in Vibrations, The Macmillan Co., New York, NY, 1967.

50. Meirovitch, L., Computational Methods in Structural Dynamics, Sijthoff & Noordhoff, The Netherlands, 1980.

51. Birchak, J. R., "Damping Capacity of Structural Materials," Shock and Vibration Digest, Vol. 9, No. 4, 1977, pp. 3-11.

The vita has been removed from the scanned document